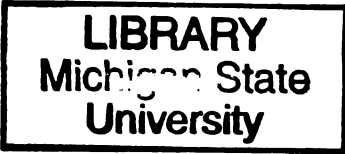




141  
466  
THS

THESIS

2  
2009



This is to certify that the  
thesis entitled

**THERMOELECTRIC CONVERSION OF WASTE HEAT TO  
ELECTRICITY IN AN IC ENGINE POWERED VEHICLE:  
AN ENGINE MODELING APPROACH**

presented by

Andrew T. Hartsig

has been accepted towards fulfillment  
of the requirements for the

          M.S.           degree in           Mechanical Engineering          

*Harold G. Ahn*  
Major Professor's Signature

          8/19/08            
Date

**PLACE IN RETURN BOX** to remove this checkout from your record.  
**TO AVOID FINES** return on or before date due.  
**MAY BE RECALLED** with earlier due date if requested.

DATE DUE	DATE DUE	DATE DUE

**THERMOELECTRIC CONVERSION OF WASTE HEAT TO  
ELECTRICITY IN AN IC ENGINE POWERED VEHICLE:  
AN ENGINE MODELING APPROACH**

**By**

**Andrew T. Hartsig**

**A THESIS**

**Submitted to  
Michigan State University  
in partial fulfillment of the requirements  
for the degree of**

**MASTER OF SCIENCE**

**Mechanical Engineering**

**2008**

## **ABSTRACT**

### **THERMOELECTRIC CONVERSION OF WASTE HEAT TO ELECTRICITY IN AN IC ENGINE POWERED VEHICLE: AN ENGINE MODELING APPROACH**

By

Andrew T. Hartsig

Approximately 60% of fuel energy is lost as heat in a modern internal combustion engine. This work provides an evaluation of the potential use of thermoelectric generators as a direct energy conversion device to produce electrical energy from the exhaust gases of a Cummins ISX 15 liter, turbocharged on-road diesel engine. The generated electricity is to be used to augment the existing engine power output through a hybrid drive system. Ricardo WAVE, an engine simulation code, was employed to create a model of the ISX engine and determine exhaust gas properties as well as heat transfer to the duct walls of the thermoelectric generator (TEG). The generated data is then used to calculate a theoretical improvement in brake specific fuel consumption (BSFC) and also as an aid to material scientists working to create a thermoelectric material suited for this application. In the modeling efforts it was established that maintaining power output levels on the engine was paramount and therefore the TEG must not interfere with turbocharger operation. The final model configuration utilized two TEGs with a small heat exchanger, yielding a BSFC improvement of 4.9% that was calculated at the “cruise” operating point (1500 rpm and 62% full engine load). This can potentially save over 4200 gallons of fuel over the emissions useful life (435,000 miles) of the engine.

## **ACKNOWLEDGEMENTS**

First of all I would like to express my appreciation to my advisor Dr. Harold Schock for the opportunity to work with him at the MSU Engine Lab. I would also like to thank him for his patience, guidance, and assistance over the past two years. Secondly I would like to thank Dr. James Novak for bringing me into this project as a summer worker which led to my enrollment in graduate school, for his assistance with WAVE, the many tangents we got onto, the reality checks, and helping to keep me on track. I would like to thank Dr. Giles Brereton for being on my committee as well as always being around for some good car discussions. Thanks also go out to Dr. Tim Hogan for being on my committee and for his assistance with this project. I must thank the people that work at the engine lab Tom, Ed, Melissa, Mayank, Mulyanto, Cody, Andrew, and everyone else who make it such an entertaining place to work. I would like to thank the late Dr. James Hannemann and family for stimulating my interest in science and engineering as a child. I owe thanks to my sister Jen for always being there to call me names. Thanks to all my friends for their continual support and distraction. And finally I would like to thank my parents George and Sandy Hartsig for raising me to question everything, think for myself and supporting me in every way. Without their help I doubt I would have been able to come to MSU in the first place.

# TABLE OF CONTENTS

LIST OF TABLES.....	vii
LIST OF FIGURES .....	viii
LIST OF SYMBOLS AND ABBREVIATIONS .....	x
1 Introduction.....	1
1.1 Project Concept and Goals.....	1
1.2 Introduction to Thermoelectrics .....	5
1.3 Fuel Costs and Engine Life.....	9
2 Introduction to Ricardo WAVE.....	12
2.1.1 Heat Transfer Considerations .....	15
2.1.2 WAVE Stick Models and Icons.....	17
2.2 Cummins ISX Engine Test Data.....	19
2.2.1 Engine Operating Points .....	19
2.3 Analysis Methods .....	21
2.3.1 WAVEpost Post-Processing .....	22
2.3.2 Excel Post Processing .....	24

3	WAVE Studies.....	25
3.1	Phase I.....	26
3.1.1	Single TEG Unit per Engine Cylinder.....	28
3.1.2	One TEG per Three Cylinders.....	30
3.1.3	One TEG Unit per Six Engine Cylinders.....	31
3.1.4	WAVE Model Validation and TEG Effectiveness.....	32
3.1.5	Optimization of TEG Design.....	34
3.1.6	Effects of Unsteady Flow Dynamics on TEG Heat Transfer.....	38
3.1.7	Overall Results for Phase I.....	41
3.1.8	Electrical Energy Utilization.....	43
3.1.9	BSFC Calculation.....	45
3.1.10	Conclusions for Phase I.....	47
3.2	Phase II.....	49
3.2.1	Expansion of Simplified Model.....	49
3.2.2	New devices and sub-models.....	49
3.2.3	Variable Geometry Turbocharger.....	50
3.2.4	Intercooler.....	53
3.2.5	EGR Circuit.....	53
3.2.6	Control System.....	55
3.2.7	Sensors and Actuators.....	56
3.2.8	WAVE Model Validation.....	57
3.2.9	Results.....	59
3.2.10	BSFC Calculation for Single TEG/EGR Cooler.....	61
3.2.11	Summary of Phase II.....	62

3.3	Phase III.....	63
3.3.1	TEG Placement Concepts .....	63
3.3.2	Dual TEG.....	63
3.3.3	TEG on Each Exhaust Port .....	67
3.3.4	TEG / EGR Cooler and Dual TEG Concepts with Heat Exchangers .....	72
3.3.5	Advanced BSFC Calculation .....	77
3.3.6	New Baseline Model.....	80
3.3.7	Updated BSFC Calculations for All Concepts .....	83
3.3.8	Summary of Phase III .....	88
4	Overall Summary.....	89
5	Conclusion .....	91
6	Future Work.....	91
	APPENDIX: VARIABLE GEOMETRY TURBINE MAPS.....	92
	REFERENCES .....	97

## LIST OF TABLES

Table 1: Summary of recent works in thermoelectrics relating to IC engines .....	3
Table 2: Analysis of "useful life" assuming 10% efficiency increase .....	11
Table 3: A sample of the test data provided by Cummins for the ISX engine .....	20
Table 4: WAVE heat transfer results for one, three, and six cylinders per TEG configurations .....	41
Table 5: Average TEG gas and wall temperatures .....	42
Table 6: BSFC percent improvement for three Phase I configurations .....	46
Table 7: Comparison of Cummins test data to WAVE model results .....	57
Table 8: Inner and outer wall temperatures for single TEG/EGR cooler concept.....	60
Table 9: BSFC percent improvement for single TEG/EGR cooler .....	61
Table 10: BSFC percent improvement for dual TEG configuration .....	65
Table 11: BSFC percent improvement for 30cm TEG duct length (un-optimized) .....	70
Table 12: BSFC percent improvement: Single TEG/EGR cooler with and without heat exchanger.....	74
Table 13: BSFC percent improvement: Dual TEG with and without heat exchanger .....	76
Table 14: Results of the new BSFC percent improvement calculation for the dual TEG study.....	78
Table 15: Comparison of percent difference between Cummins test data and baseline WAVE model .....	82
Table 16: Baseline engine model power output listed for each load point compared to Cummins test data.....	83
Table 17: Updated BSFC percent improvement for all concepts .....	84
Table 18: Summary of BSFC percent improvement .....	87

## LIST OF FIGURES

Figure 1: Sketch of a thermoelectric couple .....	5
Figure 2: Single unit TEG with detail of TE module .....	7
Figure 3: Rectangular cross-section of TEG shown in Figure 2 .....	8
Figure 4: Cummins ISX 6-cylinder diesel engine .....	10
Figure 5: Equivalent “effective” circular cross-section of TEG.....	14
Figure 6: WAVE icons for a simple single cylinder diesel engine.....	17
Figure 7: Basic icons used by WAVE. yjun2 is a complex Y-junction; yjun3 is a simple Y-junction; duct1 is a basic duct with the arrow head defining the right end .....	18
Figure 8: Six-unit TEG .....	27
Figure 9: WAVE representation of single-cylinder engine with one TEG .....	28
Figure 10: WAVE representation of 3-cylinder engine with one TEG .....	30
Figure 11: WAVE representation of a 6-cylinder engine with one TEG .....	31
Figure 12: Effect of TEG effective diameter – single cylinder case .....	35
Figure 13: Exhaust gas temperatures at TEG midpoint.....	39
Figure 14: Heat flux at TEG midpoint.....	40
Figure 15: Gas velocities at TEG midpoint .....	40
Figure 16: Architecture of the thermal power B-62 operating point .....	43
Figure 17: WAVE engine system layout of single TEG/EGR cooler configuration.....	50
Figure 18: Compressor performance map .....	51
Figure 19: WAVE icons for the VGT with components labeled.....	52
Figure 20: WAVE schematic of the intercooler .....	53
Figure 21: WAVE diagram of the EGR circuit with labels.....	54

Figure 22: Diagram comparing wall temperatures for the single TEG/EGR cooler configuration at the B-62 operating point with the Phase I six cylinders per TEG configuration .....	60
Figure 23: WAVE diagram for the dual TEG configuration .....	64
Figure 24: BSFC percent improvement comparison for single TEG/EGR cooler and the dual TEG configuration .....	66
Figure 25: WAVE stick diagram showing the 6 TEGs in the exhaust manifold.....	67
Figure 26: Plot of engine horsepower vs. TEG length for all 5 operating points.....	69
Figure 27: Plot of total TEG heat transfer vs. TEG length for all 5 operating points .....	69
Figure 28: WAVE stick diagram of single TEG/EGR cooler (length 150 cm) with additional heat exchanger (length 50 cm).....	73
Figure 29: WAVE stick diagram of dual TEG configuration (length 200 cm) with additional heat exchanger (length 50 cm).....	75
Figure 30: Comparison of the results of the new BSFC percent improvement calculation to the previous calculations .....	79
Figure 31: WAVE diagram of baseline model with heat exchanger replacing TEG .....	80
Figure 32: Comparison of BSFC percent improvement: Single TEG/EGR cooler concept with and without heat exchanger .....	85
Figure 33: BSFC percent improvement for all five concepts using new BSFC calculation .....	86
Figure 34: Turbine Performance Map VGT Rack Position 1.0.....	92
Figure 35: Turbine Performance Map VGT Rack Position 0.75.....	93
Figure 36: Turbine Performance Map VGT Rack Position 0.5.....	94
Figure 37: Turbine Performance Map VGT Rack Position 0.25.....	95
Figure 38: Turbine Performance Map VGT Rack Position 0.0.....	96

**Images in this thesis are presented in color.**

## LIST OF SYMBOLS AND ABBREVIATIONS

<u>Symbol</u>	<u>Description</u>
A-100	Operating Point: 1230 RPM @ 100% Engine Load
A-25	Operating Point: 1230 RPM @ 25% Engine Load
B-100	Operating Point: 1500 RPM @ 100% Engine Load
B-62	Operating Point: 1500 RPM @ 62% Engine Load
BHP	Brake Horsepower
Bi	Bismuth
BISG	Belt Integrated Starter/Generator
BMEP	Brake Mean Effective Pressure
BSFC	Brake Specific Fuel Consumption
C-100	Operating Point: 1800 RPM @ 100% Engine Load
CAD	Computer-Aided Design
CAE	Computer-Aided Engineering
CCD	Charge-coupled Device
$C_f$	Coefficient of Friction
EGR	Exhaust Gas Recirculation
ESC	European Steady-State Cycle
Ge	Germanium
HP	Horsepower
IC	Internal Combustion
N	N-type Thermoelectric Leg
NO <sub>x</sub>	Nitrogen Oxides
$N_{TEG}$	Number of Thermoelectric Generators
OTR	Over-the-Road
P	P-type Thermoelectric Leg
QTEG	Gas Side Heat Transfer to TEG Duct Wall
RPM	Revolutions per Minute
RTGs	Radioisotope Thermal Generators
Si	Silicon
TE	Thermoelectric
Te	Tellurium
TEG	Thermoelectric Generator
VGT	Variable Geometry Turbocharger
$\eta_{BISG}$	Belt Integrated Starter/Generator Efficiency
$\eta_{INV}$	Inverter/Power Electronics Efficiency
$\eta_{TEG}$	Thermoelectric Generator Efficiency

# **1 Introduction**

## **1.1 Project Concept and Goals**

Currently the best internal combustion (IC) engines have brake efficiency of 40%, with 35% of the fuel energy going to exhaust, and 25% to other heat transfer losses such as the cooling system. Thus in the best IC engines, 60% of the energy content in the fuel is rejected as heat. As transportation fuel costs continue to rise, new technologies are needed which will improve fuel efficiency.

This work provides an evaluation for the potential use of thermoelectric materials implemented in a direct energy conversion device to produce electrical energy from the exhaust gases of a Cummins on-road diesel vehicle powerplant. The generated electricity will be used to augment the existing engine power output through a hybrid drive system and will therefore decrease overall fuel consumption. While the maximum amount of energy recovery may take place at the peak power output of the engine, road vehicle engines do not typically operate at peak power for extended periods of time and therefore more realistic operating conditions must be studied to evaluate the potential energy recovery.

Recently several groups have investigated the use of thermoelectric devices to capture waste heat from the exhaust of IC engines. A few relevant findings of these efforts are discussed below and a summary is listed below in Table 1.

Kushch et al. at Hi-Z Technology Inc., a manufacturer of thermoelectric devices, have been experimenting with thermoelectric devices on IC engines since at least the year 2000. Hi-Z has been successful in utilizing 72 of their TE modules to construct a TEG generating 1 kW of electrical power at 30 V DC. The testing was conducted on a dynamometer fitted with a Cummins 335 HP Diesel engine. The Hi-Z experiment found that the TEG power output strongly depended on engine loading and less on the engine speed. [1]

Ikoma et al. with Nissan Motor Co. have experimented with integrating TE devices to capture exhaust heat before the catalytic converter. Using 72 Si-Ge TE modules of their own design, they were able to generate nearly 36 W of electrical power. The testing took place on a combustor test rig which approximated the exhaust gas temperature and flow rate of a 3 L gasoline engine performing a 60 km/hr hill climb. The testing determined that the generated power was 0.9% of the heat flux from the exhaust gas to cooling water. They concluded that further improvements are needed to prevent heat transfer around the TE modules, and the conversion efficiency of the modules also needs improvement. [2]

Work by Matsubara et al. at the Science University of Tokyo in Yamaguchi has also explored the use of thermoelectric generators to extract energy from exhaust gases of an IC engine. This group was heavily involved with developing new TE materials for operation in the 350-750°C temperature range. Experimental testing of their new materials took place on a 2 L gasoline engine in a Toyota Estima. The TEG was constructed of 6 segmented modules (skutterudites /  $\text{Bi}_2\text{Te}_3$ ) and 4 HZ-14 modules from

Hi-Z Technology, Inc. The testing took place with the engine driving the vehicle at 60 km/hr. The system initially produced electrical power of 141 W (at 22.4 V and 6.29A) and after modification the system was able to produce 266 W of electricity. They concluded that the power generated was approximately half of the potential of the TEG and that poor thermal conductivity between the exhaust gas and the TE modules was the cause. [3]

A review paper produced by Vazquez et al. (Universidad Pontificia Comillas in Madrid, Spain) researched works over the previous three decades concerned with thermoelectric devices utilizing exhaust heat energy from IC engines. This work provided a useful breakdown of other works into multiple categories and providing comparisons between works. This work concludes that the transfer of heat from the exhaust gas to the TE modules is the primary obstacle to high performance in TEGs. [4]

**Table 1: Summary of recent works in thermoelectrics relating to IC engines**

Recent work	Description of work	Assessment
Hi-Z [1]	HiZ-1kW Generator for Diesel, 1kW, 5% efficiency, ~600C exhaust gas, but only 250-275C hot side, water cooled cold	~600C Exhaust gas and 250-275C hot side suggests poor performance of heat exchanger
Nissan [2]	36W generator, 1% efficiency, 595C Exhaust gas, Si-Ge	They concluded poor performance of heat exchanger and significant parasitic heat loss from module
Matsubara et al.[3]	266 Watts from 2.0 Liter engine, Skutterudite-BiTe, ZT~1 at 800C, Exhaust gas ~650C, but hot side only 450C, and cold side 150C despite water cooling at 25C	They concluded poor heat exchanger performance- ~200C drop from exhaust temp to hot side and ~125C drop on cold side. TE generator performance 50% of what was expected as a result of poor heat exchanger.
Vazquez et al. [4]	Significant experience with TE generators	Critical component of waste heat recovery is heat exchanger efficiency.

The work presented within is a component of a greater DOE Project under way at MSU in conjunction with Iowa State University, NASA Jet Propulsion Laboratory, Cummins Engine Company and Tellurex Corporation. Previous works were primarily focused on experimental testing of TE devices. This work makes use of the engine simulation software WAVE developed by Ricardo to predict gas and duct wall temperatures and heat transfer rates at various locations on the engine. The temperature and heat transfer data generated by WAVE is used in conjunction with a simple thermoelectric generator (TEG) model to estimate the improvement to the brake specific fuel consumption (BSFC) of the powertrain.

## 1.2 Introduction to Thermoelectrics

Currently, thermoelectric devices are commonly used in a variety of cooling and power generation applications. They are fully reversible heat pumps, such that when electrical current is supplied to the device, a temperature gradient is established, and when a temperature gradient is supplied across the device, electrical current will flow (if a load resistance is attached).

Thermoelectric generators (TEG) are constructed of a large number of thermoelectric (TE) couples joined together thermally in parallel and electrically in series. A diagram of a TE couple can be seen in Figure 1. Traditional uses include cooling electronics such as infrared detectors, laser diodes for fiber optics, and CCD arrays, as well as power generation applications such as radioisotope thermal generators (RTGs) used on Apollo 12, 14, 15, and 17, Voyager I and II, Galileo, etc. [5]

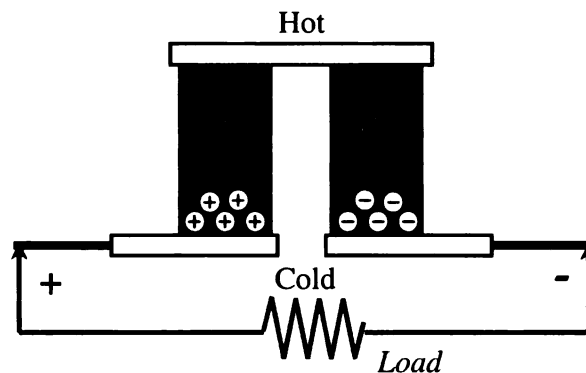


Figure 1: Sketch of a thermoelectric couple

There are a number of advantages for thermoelectric devices over competing technologies, including:

- High reliability (> 250,000 hrs)
- Silent and no vibration
- Small electromagnetic signature
- Temperature control to fractions of a degree
- Not position-dependent
- Function in environments too severe, or too sensitive to conventional refrigeration
- Small and lightweight
- No chlorofluorocarbons, chemicals, or compressed gases (nothing to replenish)
- Environmentally “green”
- Direction of heat pumping is fully reversible

The most significant disadvantage of thermoelectrics is their relatively low efficiency. A broader related study at MSU focuses on increasing this efficiency by using longer legs, higher temperature gradients, segmented legs, and new materials and fabrication techniques.

As noted above, consideration of the possible sources of “waste heat” from diesel engines led to the conclusion that the exhaust gases are the highest in energy and most easily accessible by TEGs. Their use offers the further benefit of replacing the existing exhaust gas recirculation (EGR) cooler with the TEG, thus enabling effective NO<sub>x</sub> emissions control.

Figure 2 shows one proposed design of what will be referred to here as a single TEG which could be used in the exhaust system. The hot exhaust gas would flow through the center passage and engine coolant would flow through the outer two passages similar to counterflow heat exchangers. The thermoelectric modules are sandwiched between the hot exhaust passage and the coolant passage on each side of the device. This initial overall TEG design resulted from CAD “packaging” studies with the intent of fitting a sufficient number of P-N modules into a single TEG unit to produce approximately 1 kW of power. This was based on certain “best estimates” of P-N junction dimensions and efficiencies.

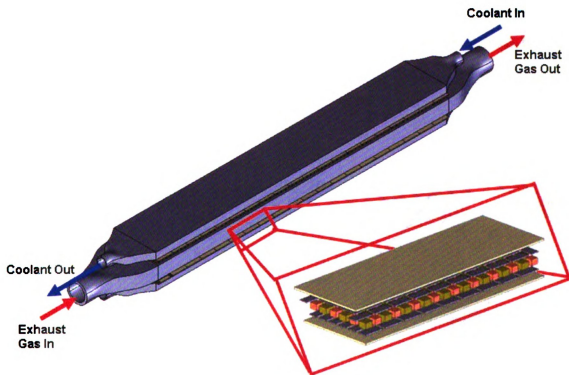


**Figure 2: Single unit TEG with detail of TE module**

As illustrated in Figure 2, exhaust gases from the engine exhaust ports, or the exhaust manifold outlet (depending on the type of application, as discussed below), enter the left

end of the TEG unit and exit on the opposite end. Similar to a counterflow heat exchanger, liquid coolant enters on the right, through separate ducting, and exits on the left. Also shown is an enlarged picture of a P-N “Module” which includes 54 P-N junctions. In the figure, 40 of these modules (20 each on the top and bottom) make up the entire TEG “Unit” shown. Note that the overall length of the TEG Unit, which is a key design variable as shown below, will determine the total number of modules.

Figure 3 below shows a cross-section of the Single Unit TEG from Figure 2. The TEG assembly is sandwiched with aluminum heat exchangers through which engine coolant flows. The central duct, where the exhaust gas will flow, is constructed of stainless steel. The P and N legs of thermoelectric material are electrically isolated from the heat exchangers with aluminum nitride pads which also provide thermal conductivity between the components.

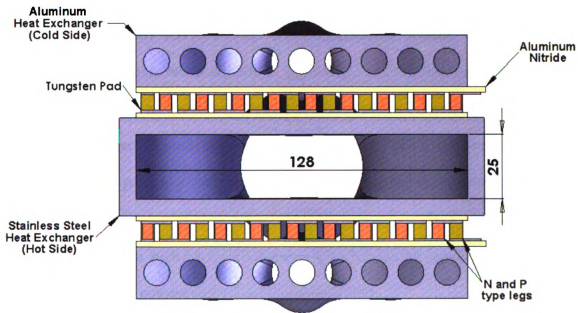


Figure 3: Rectangular cross-section of TEG shown in Figure 2

### **1.3 Fuel Costs and Engine Life**

There were two Cummins engines originally considered for use in this project. Both are inline 6-cylinder, direct injected, turbocharged, and utilize cooled EGR for emissions control.

The first is the Cummins ISB engine. This engine has a displacement of 5.88 L, and the bore and stroke are 102 mm and 120 mm respectively. This engine also employs a computer-controlled high-pressure common rail fuel injection system. This base engine, in various configurations, is utilized in many applications. These applications include marine, construction and agricultural, recreational vehicles, medium duty trucks and busses, electrical power generators, and the Dodge Ram pickup truck.

The second is the Cummins ISX engine. This engine has a displacement of 14.95 L with a bore of 137 mm and a stroke of 169 mm. The primary application of this engine is Class 8 over-the-road (OTR) trucks. Other applications include construction and agricultural equipment, electrical power generation, and recreational vehicles. This engine employs many new technologies found in modern diesel engines such as computer controlled unit injectors, variable geometry turbocharger (VGT), and cooled EGR. The EGR system is of particular interest for this study because the ISX engine uses an EGR cooler to lower the temperature of the exhaust gas before it is mixed into the intake air charge. This offers a prime location where waste heat energy could be captured and reintroduced into the powertrain by use of thermoelectrics.



**Figure 4: Cummins ISX 6-cylinder diesel engine**

The aim of this project is to improve fuel economy in an on-road application. Two common applications considered were the Dodge Ram pickup truck with an ISB engine and a typical Class 8 OTR truck with an ISX engine. A comparative analysis was conducted to determine which engine (ISB or ISX) would be the most economically viable to implement the thermoelectric generator device.

An engine / powertrain efficiency gain of about 10% in either the ISX or ISB engines would be considered a very significant improvement. According to Cummins, the engines have an emissions “useful life” as defined by emission regulations. The emissions equipment must function properly for the duration of the “useful life”. The “useful life” of the ISB and ISX engines is 185,000 and 435,000 miles respectively. Table 2 shows simple analysis of the “useful life” based upon emissions regulations, estimated cost of fuel, some typical fuel economy expectations, fuel savings, and associated monetary savings.

**Table 2: Analysis of "useful life" assuming 10% efficiency increase**

	ISB Dodge Pickup	ISX Class 8 Truck
Emissions – Useful Life	185,000 miles	435,000 miles
Typical Fuel Consumption	16 mpg	5 mpg
Fuel Consumed During Useful Life	11,500 Gallons	87,000 Gallons
Fuel Consumed with 10% Improved Efficiency	10,500 Gallons	79,100 Gallons
Fuel Saved	1,000 Gallons	7,900 Gallons
Money Saved (\$4.00/Gal April 2008)	\$4,000.00	\$31,600.00

It is clear from the analysis that the ISX engine will see a greater overall fuel and cost savings from an increase in fuel efficiency. The greater savings will be needed to help offset the additional cost of the TEG device. If the fuel savings will not be able to offset the cost of the device it would be very difficult to market such a device successfully.

## **2 Introduction to Ricardo WAVE**

Early in the proposal phase of this project, it was determined that an engine simulation code would be essential to the success of the project as a whole. Through the use of the simulation code, gas and wall temperatures as well as heat flux can be predicted. This data is useful to the TE materials group in developing and selecting materials which perform optimally at the operating conditions of the engine. WAVE is one such engine performance simulation code. It is a commercially available CAE tool which has been utilized in industry for over twenty years in the development of internal combustion engines. One of the primary uses of this code is to aid in the design of intake and exhaust system components at various engine loads and throttle conditions. WAVE was chosen because it provides a reasonable simulation of the complex interactions found in an IC engine. Wave dynamics can have a significant effect on engine operation. Wave dynamics are pressure waves propagating through gases as they move through ducts. These pressure waves can be reflected back in the duct by abrupt changes in cross-sectional area (Duct to plenum junctions, opening/closing of valves, etc.). WAVE also has the capability to simulate many of the complex components found on the ISX engine (turbochargers, intercoolers, heat exchangers, etc.). The following section covers the theory of operation and use of this software.

## **2.1 Theory of operation**

WAVE utilizes a one-dimensional approach to solving the partial differential equations governing the gas flow throughout the intake and exhaust system ducting of the engine. While the governing equations are mathematically one-dimensional (with the spatial axis along the centerline of the duct) it has many parameters which take into account three-dimensional effects such as changes in duct cross-sectional area, bends and other flow losses. In addition, substantial conductive and convective heat transfer models are employed in WAVE. The primary reason behind the quasi-1D approach is that in a fully 3D code the computer calculation time can be prohibitively long. By using a quasi-1D formulation, WAVE is able to provide results on a cycle-averaged basis, which is quite useful when the extremely detailed thermo-fluid flow characteristics of a conventional 3D simulation are not required. Therefore, this type of quasi-1D code is the primary type of CAE tool utilized in industry for studying the effects on engine performance and fuel consumption from various engine design changes.

Although the preferred TEG construction shown in Figure 3 cannot be directly modeled with the Quasi-1D approach, WAVE does allow one to account for most design features of interest, such as the non-circular duct cross-section shape and its attendant increased wall wetted surface area for heat transfer. Figure 5 illustrates how the rectangular TEG cross-section (perpendicular to the gas and coolant flow directions) would be represented within WAVE as a circular cross-section of the same “effective” flow and wetted wall areas (Figure 3). The circular duct is surrounded by TEG modules which are then surrounded by the engine coolant heat exchangers.

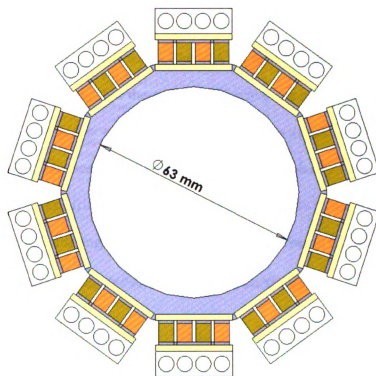


**Figure 5: Equivalent “effective” circular cross-section of TEG**

### 2.1.1 Heat Transfer Considerations

Noted previously, one of the major challenges in integrating a TEG into an IC engine exhaust system is the effectiveness of the heat exchanger. In order to meet requirements for TEG performance, the convective heat transfer from exhaust gas to TEG duct wall must be increased. The following excerpt from the WAVE Basic User Manual [7] discusses heat transfer multipliers applied to the convective heat transfer to duct walls.

The user may optionally multiply the calculated values of  $C_f$  depending on wall roughness. The multiplier should be set to unity for smooth walls and to larger values for rough walls. The WAVE heat transfer model assumes the Colburn analogy; that the transport of scalar quantities (such as heat) follows a similar law to that for vector quantities (such as momentum). Accordingly, the heat transfer multiplier should typically have the same value as the skin friction multiplier. One exception is in the modeling of intake and exhaust engine ports where  $C_f$  should be set to 0.0 because wall friction is already included in the valve flow coefficients.

Normally WAVE suggests a value of 2.0 for the heat transfer multiplier for exhaust ducts. This assumes that most exhaust ducts will have a rough inner surface which will increase the convective heat transfer due to turbulence.

Work conducted by Shih et al. at Iowa State University, a partner in the DOE project, has shown that the use of pins, ribs, dimples or a combination of the three will significantly enhance the heat transfer over that of a smooth wall. They predict that in our model we

can assume that by using additional heat transfer enhancements we can increase the heat transfer by up to 5 times over a simple rough wall. Combining the 5 times enhancement with the 2 times multiplier from the rough surface, we assumed that ideally we will have a 10 times heat transfer multiplier which will be used in the convective heat transfer calculation for the TEG duct walls. [6]

For further detail on heat transfer in the WAVE model refer to the WAVE Basic, Engine, and Conduction Manuals [7],[8],[9].

### 2.1.2 WAVE Stick Models and Icons

This section is a brief introduction to how WAVE displays the layout of the engine in its preprocessor. WAVE uses icons to represent the various components found in the engine, and this brief introduction will help familiarize the reader with the icon system which appear later in this document in multiple figures. Every component has an associated dialog box where parameters of that component are specified.

Figure 6 below contains icons for a special type of junction which represents an engine cylinder, two ambients, two orifices and several ducts. Ducts are represented by solid black lines with an arrow head on one end (labeled as IntDuct, IntPort, ExhPort and ExhDuct in Figure 6). The arrow head on the duct is used to designate the right end of the duct, not the flow direction. This left to right convention is used regardless of the orientation of the duct on the canvas and is primarily used when ducts have a taper along their length. The blue circle on the left side of the EngineCylinder junction in Figure 6 represents the intake valve. The red circle on the right represents the exhaust valve.

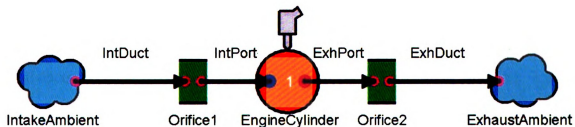
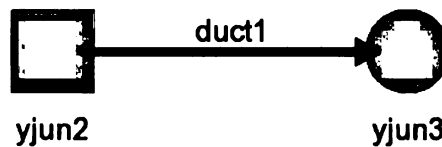


Figure 6: WAVE icons for a simple single cylinder diesel engine

Ducts representing ports (IntPort and ExhPort) are used to connect the valves to the orifices (Orifice1 and Orifice2) which then have ducts (IntDuct and ExhDuct) connecting out to the ambients (IntakeAmbient and ExhaustAmbient). By default the diameter of an orifice automatically matches that of the ducts which connect to it. The diameter of an

orifice can also be specified to any diameter from 0 to the diameter of the ducts which connect to it. This variable orifice diameter is often used to model a simple valve. At the top of the cylinder junction is an icon which represents a fuel injector, this may be placed directly into cylinder junctions, ducts, or Y-junctions depending on the engine configuration.

Figure 7 shows a basic duct (duct1) connecting a complex Y-junction (yjun2) to a simple Y-junction (yjun3).



**Figure 7: Basic icons used by WAVE. yjun2 is a complex Y-junction; yjun3 is a simple Y-junction; duct1 is a basic duct with the arrow head defining the right end**

Simple Y-junctions allow multiple ducts to connect together without needing to specify the exact orientation of each duct. It is assumed that the ducts are evenly separated on a virtual spherical volume. Complex Y-junctions allow for much greater control over how ducts connect together including angles between ducts and volume of junction, in addition to allowing a special type of duct called a multiple duct which consists of several small ducts all connected in parallel which is useful for heat exchanger modeling. Special icons are introduced later as the associated components are integrated into the WAVE models.

## **2.2 Cummins ISX Engine Test Data**

Cummins Inc. supplied experimental and design data on their ISX engine. Cummins tests their heavy duty OTR diesel engines at 5 operating points as defined by the ESC (European Steady-State Cycle). These operating points represent the 5 of the more typical driving situations that the engine will experience. Experimental data are collected at these 5 operating points on an engine dynamometer. This includes engine output (torque) as well as data gathered from sensors in various locations around the engine yielding gas temperatures and pressures. Additionally, critical values such as fuel rate, air flow rate and EGR mass flow have been measured. Cummins also supplied a great deal of design information about the ISX engine including, basic geometry of the engine (bore and stroke), intake and exhaust manifold geometry, fuel injection profiles, valve lift profiles and other important factors to the modeling effort.

### **2.2.1 Engine Operating Points**

The operating points are designated by a letter and a number. The letter corresponds to the engine speed and the number is the percentage load on the engine. Five operating points are of interest consisting of three engine speeds of: (A) 1230 rpm, (B) 1500 rpm, and (C) 1800 rpm. Each of the three engine speeds is tested at full (100%) load. Two operating points are considered to be “part load”, 25% of full load at 1230 rpm (A-25), and a 62% of full load at 1500 rpm (B-62). The B-62 operating point is the focus of much interest as this is designated as the “cruise point” by Cummins. This is the operating point where a truck has a full trailer and is cruising at a steady highway speed. Cummins has gone to great lengths to make the B-62 point as fuel-efficient as possible for this is how the engine will spend the majority of its useful life. In the WAVE simulation, engine load

is regulated by controlling the fuel rate. The fuel rate for the five operating points was provided by Cummins, and the fuel injectors in WAVE were set to deliver the specified fuel rate regardless of how the rest of the engine is performing. Therefore, if the power output of the model is similar to that of the experimental engine, it can be assumed that the model is performing accurately. Table 3 below displays a sample of the test data provided by Cummins. The five columns on the right show the data for each of the five operating points.

**Table 3: A sample of the test data provided by Cummins for the ISX engine**

<b>Modes</b>	<b>Units</b>	<b>A-25</b>	<b>A-100</b>	<b>B-62</b>	<b>B-100</b>	<b>C-100</b>
<b>Engine Crankshaft Speed</b>	rpm	1230.00	1230.00	1500.00	1500.00	1800.00
<b>Torque</b>	ft-lb	472.15	1886.80	1170.20	1887.30	1577.70
<b>BMEP</b>	psi	78.05	311.92	193.45	312.00	260.82
<b>Power</b>	HP	110.58	441.88	334.22	539.02	540.72
	kW	82.46	329.52	249.23	401.96	403.22
<b>Fuel Rate</b>	lb/hr	40.30	147.76	111.88	183.56	196.64
	kg/hr	18.28	67.02	50.75	83.26	89.20
<b>Air Flow Rate</b>	lb/min	19.81	47.78	46.71	63.55	68.42
<b>Fuel-Air Ratio</b>		0.034	0.052	0.040	0.048	0.048
<b>EGR Mass Flow</b>	lb/min	7.18	9.87	12.80	15.96	13.22
<b>EGR Fraction of Intake Charge</b>		0.27	0.17	0.22	0.20	0.16
<b>Barometer</b>	Hg abs	29.43	29.43	29.43	29.43	29.44
<b>Intake Manifold Pressure</b>	Hg abs	13.90	61.21	46.19	73.57	62.38
<b>Intake Manifold Temperature</b>	°F	120.07	121.78	114.42	130.47	135.12
<b>Exhaust Manifold Pressure</b>	Hg abs	18.37	70.19	54.14	85.95	79.61
<b>Exhaust Manifold Temperature</b>	°F	733.27	1170.90	945.27	1159.60	1233.60

### **2.3 Analysis Methods**

WAVE has some features which are very useful in experimenting with model changes: constants, cases and subcase sweeps. Constants allow the user to specify a name for a particular numerical value. These names are then linked to a constants table which can contain several cases. Cases are normally used to switch the state of the model to investigate some change to the model. WAVE re-runs the simulation for each case specified. Most commonly, cases are used to specify engine speeds, and in the case of this project, the five operating points supplied by Cummins.

The constants table is arranged much like a spreadsheet and will have the various constants set to each row and the different cases assigned to the columns. In addition to the engine speed the fueling rate, boost pressure, injection timing and many other values supplied by the Cummins test data are stored in the constants table. Subcase sweeps let the user specify multiple values for a constant, usually by specifying the number of subcases and the upper and lower bounds of the range and letting the software evenly divide the range of values. When WAVE runs subcases, it will run each combination of case and subcase. For example, if there are 5 cases and a subcase sweep contains 10 different values, WAVE will run the simulation a total of 50 times in order to generate data for each combination. WAVE will allow subcases to be specified for up to two constant names. This can be quite useful when trying to find a combination of two values which yield a desired result. Running subcase sweeps will generate a large amount of raw data, particularly when two constant subcase sweeps are run concurrently. This can be

particularly cumbersome to analyze because WAVE stores much of the data in a text format.

Like most computer simulation work the post-processing of data takes as much if not more time than the setup of the model. Fortunately WAVE is bundled with a post-processor called WAVEpost which is quite effective at generating 2D and 3D plots for any number of variables. Unfortunately WAVEpost is not ideally suited to certain aspects of analysis particularly when a single cycle-averaged number is needed. For these situations, a combination of text editors and Microsoft Excel work quite well.

### **2.3.1 WAVEpost Post-Processing**

WAVEpost 2D plots are generated in two basic formats; time/engine cycle based and sweep plots. WAVEpost will automatically generate several default time/engine cycle plots covering a wide variety of engine performance and operation. If any time plots were specified in the preprocessor, WAVEpost will also automatically construct those plots. It is quite easy to create plots for case and subcase sweep studies. It is also possible to add a secondary ordinate to plots in order to plot two different sets of data against a common x-axis, for example torque and horsepower vs. engine speed.

Engine cycle plots are useful for studying phenomena such as wave dynamics or temperature variation over a finite time period. Time-based plots are good for exploring transient behavior like duct wall temperature variation. Sweep plots are used in conjunction with either case or subcase constant sweeps, where the value being varied

(RPM, duct diameter, etc.) would be used as the x-axis and the dependent variable on the y-axis.

Additionally, WAVEpost allows for 3D plots that are very useful in analyzing data obtained from subcase sweeps of two constants (a double sweep). When a double sweep is conducted, it is similar to the multiplying effect discussed above on cases and subcases; but in many situations a much higher number of simulations will result. For example, if two constants each have 10 subcases, that will require 100 simulations for a single case. Now if that same setting is simulated for 5 cases that will require 500 simulations to generate data for each possible combination. Double sweeps are usually limited to a single case to reduce calculation time and to make the analysis much easier. A 3D plot can be generated, for example, with the two constants of a subcase sweep assigned to the x and y-axes and some value like horsepower on the z-axis.

WAVEpost also allows for complete customization of the plot by changing the axis scales, line type, colors, line size, and many other parameters in order to display the data conveniently. WAVEpost can, in addition to outputting directly to a printer, save the plot in a variety of digital formats.

### **2.3.2 Excel Post Processing**

While WAVEpost is quite effective for plotting, it can be lacking when singular averaged values are desired. A useful alternative was found in a combination of a text editor, in this case Microsoft Notepad, and Microsoft Excel. The data is structured in the .sum text file such that it displays all output data for each case before continuing on to the next case. This case by case text block organization allowed the use of the find feature in Notepad to search for the name of a particular value, such as TORQBR (Torque in ft/lbs), and when the search was continued on from that point the next case's value would be highlighted. When values were identified they were copied into a spreadsheet organized such that the values were easily compared case to case. In addition, functions were written in Excel which automatically calculates the percent difference between two values. This was used extensively when trying to match the model's output variables to those values in the experimental test data.

### **3 WAVE Studies**

This chapter focuses on the modeling efforts conducted in WAVE. The chapter is divided into three phases, ranging from a simplified model used for preliminary studies to advanced models exploring alternative configurations with the goal of improving the BSFC of the Cummins ISX engine. Phase I contains a section of work previously conducted by Dr. James Novak who is a visiting professor at Michigan State University. The author became involved in Phase I at the section titled Optimization of TEG Design. This previous work section of Phase I has been included to provide an introduction to the advanced modeling efforts of Phases II and III conducted by the author.

### **3.1 Phase I**

Phase I of the WAVE studies were conducted with a simplified model approach to determine early in the project the amount of heat energy available. Critical information obtained included the gas and wall temperatures in the TEG which will be used in conjunction with the thermoelectric group to determine the best thermoelectric material for this application. The Phase I modeling effort was focused only on the B-62 load point (1500 RPM, 62% load), which is where this engine will be operated for the majority of its useful life. Therefore this operating point is the most important in terms of fuel consumption.

There are three basic options to consider in determining how best to configure one or more of the single TEG units, shown in Figure 2, into the exhaust system of the ISX 6-cylinder engine (see Figure 4):

1. One single unit TEG per each cylinder – six units for the 6-cylinder ISX engine. This configuration might be best for packaging the largest number of P-N modules per engine; hence, generating the most electrical power. Figure 8 illustrates one such configuration.
2. One TEG unit per 3 cylinders (two TEG units per engine). This case seems to be a very reasonable alternative, because it would provide for three, equally spaced (in time) exhaust gas “pulses” to each TEG unit per engine cycle (two engine crankshaft revolutions). This follows from a consideration of the firing order of the ISX engine and the fact that the interval between the opening events of each cylinder’s exhaust valves is 120 crankangle degrees.

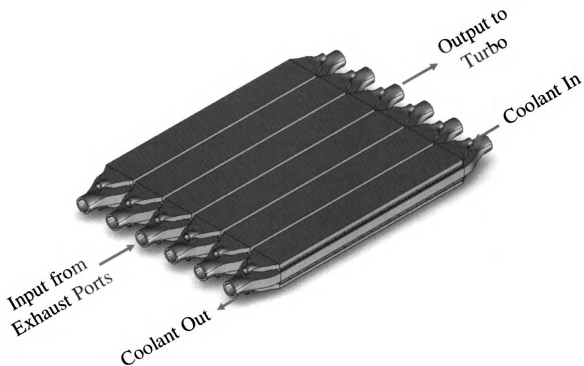


**Figure 8: Six-unit TEG**

3. One TEG unit per six engine cylinders. This configuration would entail only one TEG unit for the entire engine and would provide the highest frequency of exhaust pulses to the TEG per engine cycle – three pulses per revolution; six per engine cycle. Although the heat loading to the TEG would be the highest of any configuration, the number of P-N modules that would be exposed to this energy input would be the least due to simple packaging considerations.

### 3.1.1 Single TEG Unit per Engine Cylinder

For this configuration, in which each cylinder exhausts into its own TEG, experiments have shown and WAVE modeling results confirm that at engine speeds below 2000 rpm a 6-cylinder engine behaves as six independent single cylinder engines. Therefore, the case of six TEGs (one per cylinder) was effectively modeled as a single cylinder engine and, as necessary, displacement-specific results (e.g., torque and horsepower) multiplied by a factor of six. Figure 9 shows the simple single cylinder stick model used. This assumption decreases the computer processing times by over a factor of six and allows more extensive design optimization studies to be carried out in a practical way.

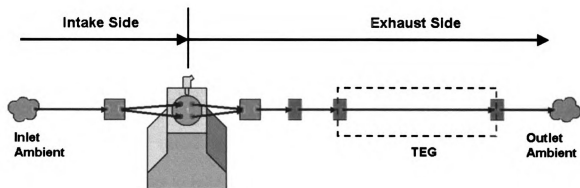


Figure 9: WAVE representation of single-cylinder engine with one TEG

In this figure, flow through the engine is from the left inlet ambient (shown as a blue “cloud”) to the right exhaust ambient. Note that an ambient corresponds to an infinite volume plenum for which thermodynamic properties, such as pressure, temperature, and gas composition, remain fixed at specified values during the entire simulation. These conditions can be those of the true ambient (i.e., atmospheric conditions), or they can represent other locations in the engine’s intake and exhaust systems where conditions are

approximately constant with time and are known; e.g., from experimental data for the operating conditions of interest. The latter case can be useful to simplify the model and avoid having to calibrate and “carry along” computations for parts of the intake and/or exhaust systems that do not have a significant effect on the results of interest.

In this study, we make use of this approximation to avoid the complexities of modeling the variable geometry turbocharger of the Cummins ISX engine. Instead, we use the measured values of pressures and temperatures: (1) at the outlet of the turbocharger compressor and intercooler (intake manifold pressure and temperature in Table 3); and (2) the inlet to the turbocharger turbine (exhaust manifold pressure and temperature in Table 3); to represent the inlet and exhaust ambient conditions, respectively.

Another important assumption used throughout this initial study of TEG behavior in IC engine exhaust systems, is that all of the exhaust gas expelled from the cylinders passes through the TEG(s) before entering the exhaust ambient (turbine inlet). As a consequence, the results to follow represent an ideal “upper bound” on the amount of energy that can be extracted by the TEGs. In the actual case of the ISX engine, up to 50% of the exhaust gas will be bypassed through the TEG/EGR cooler and the rest will enter the turbine inlet. The turbine efficiency ultimately depends on the total enthalpy of its inlet gases. This delicate balance of energy distribution within the ISX exhaust system will depend strongly on the location and design of the TEG and of the turbocharger/intercooler.

### 3.1.2 One TEG per Three Cylinders

Similar to the assumptions discussed above and confirmed by modeling studies, this configuration effectively behaves as two independent three cylinder engines coupled mechanically, but independent in terms of the flow dynamics in the exhaust system. It can, therefore, be modeled as one 3-cylinder engine to facilitate shorter computer processing times and, hence, more practical design optimization studies. Figure 10 shows the model used in the analysis below.

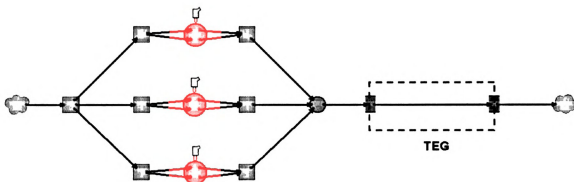


Figure 10: WAVE representation of 3-cylinder engine with one TEG

### 3.1.3 One TEG Unit per Six Engine Cylinders

Figure 11 shows the WAVE representation of this last configuration of interest. All six cylinders merge on the exhaust side into a single TEG duct. This case required the greatest CPU times, since all cylinders had to be modeled to predict the heat loading on the TEG and the output of the engine accurately.

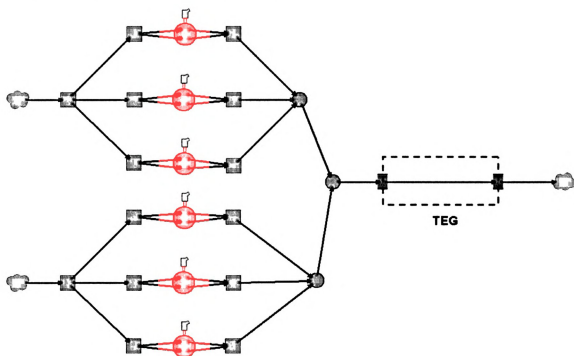


Figure 11: WAVE representation of a 6-cylinder engine with one TEG

### **3.1.4 WAVE Model Validation and TEG Effectiveness**

#### Validation for Base Engine

The WAVE code was first used to simulate the baseline ISX production engine at the B-62 operating point to validate model results for engine output. The detailed input included:

- Intake and exhaust valve lifts at one crankangle degree intervals
- Intake and exhaust valve/port flow coefficients at 1mm valve lift intervals
- Combustion energy release profile
- Base engine design parameters (bore, stroke, connecting rod length, valve diameters, compression ratio)
- Centerline lengths and cross-sectional diameters of all intake and exhaust ducting (ambient to valve seat)
- Operating conditions (B-62 “cruise point.”)

The predicted value of engine BMEP was 210 psi. This is approximately 8.5% higher than the experimental value of 193.45 psi listed in Table 1. A value within 10 percent of experimental data was considered acceptable, especially in light of the somewhat idealized intake and exhaust system designs, which did not include the details of the turbocharger compressor and turbine. Flow and heat transfer losses throughout the actual engine’s extensive induction and exhaust system components will typically reduce shaft output approximately 10 percent. As such, this baseline level of engine output was considered well within the accuracy of engine simulation codes.

### Approach Used to Evaluate TEG Effectiveness

Once it was determined that the code was simulating the base engine output in a reasonable manner, the single, three, and six cylinder TEG configurations were evaluated to determine which is the most effective in extracting exhaust heat energy. To simulate a “best case” scenario, several assumptions were incorporated into the engine-TEG system:

1. The engine piston, cylinder liners, and cylinder head combustion chamber surfaces were near adiabatic. This was accomplished by reducing the gas side heat transfer coefficients by 99%. This would be similar to using ceramic or other insulating coatings on these surfaces.
2. The exhaust ports and manifold were similarly assumed to be heat insulated to maximize the heat input into the TEG duct.
3. The TEG coolant temperature was assumed to be a constant value of 325 degrees Kelvin along its entire length. In actuality the coolant temperature will increase along its length, but this is of secondary importance in the resulting total exhaust heat extraction through the TEG structure.
4. The walls of the TEG are made up of two homogeneous layers. The inner gas-side layer is carbon steel, 3.175 mm (1/8 inch) thick, with a thermal conductivity of 48 W/m/K; and the outside layer represents the P-N modules with a thickness of 11mm and thermal conductivity of 3 W/m/K.

These assumptions allow for the maximum exhaust heat loading of the TEG, and the following results thereby represent an upper bound to the energy that would be available for conversion to electrical power.

### **3.1.5 Optimization of TEG Design**

Figure 3 above contains the key dimensions for the baseline geometry of the single unit TEG. This configuration was used as the starting point to determine an “optimized” design for the single, three, and six cylinder cases, by simulating the engine operation at the B-62 point for a range of TEG cross-section diameters and lengths. The primary output variable of WAVE, used as a measure of the TEG effectiveness in these studies, was the total heat transferred per unit time through the walls of the TEG duct during an engine cycle, denoted “DHTEG1” (units of kilowatts) by the code. This variable is calculated within WAVE by integrating the gas-side heat flux, which depends on the instantaneous values of wall and gas temperatures and the instantaneous heat transfer coefficient, over the duct’s internal surface area at each instant. The final number reported by WAVE represents a cycle-averaged value. The optimizations that follow are based on finding the maximum value of DHTEG1 as a function of key design parameters and subject to certain constraints, such as maintaining engine output (BMEP), TEG packaging limitations, etc. BMEP is used as the measure of engine shaft output, instead of brake torque, because it normalizes the output with respect to engine displacement; i.e., it is independent of the number of engine cylinders.

The interior (exhaust gas-side) cross-section diameter was found to be the most important design variable for the TEG, because it has a direct effect on the engine output, as well as the amount of heat transferred from the exhaust gases. It was considered important in these studies to avoid any significant degradation of the ISX engine output by the introduction of the TEG in its exhaust stream; e.g., by increasing the exhaust flow

restriction losses. Such a reduction in BMEP would ultimately have a detrimental impact on the engine's fuel efficiency and emissions by necessitating an increase in engine displacement to meet load requirements.

For the single cylinder case (one TEG per cylinder), Figure 12 shows the effect of changing the TEG interior (exhaust gas-side) cross-section diameter on both the engine BMEP (right-hand scale) and the total heat energy lost from the exhaust gases to the surrounding TEG wall surfaces per unit time during an engine cycle, DHTEG1 (left-hand scale).

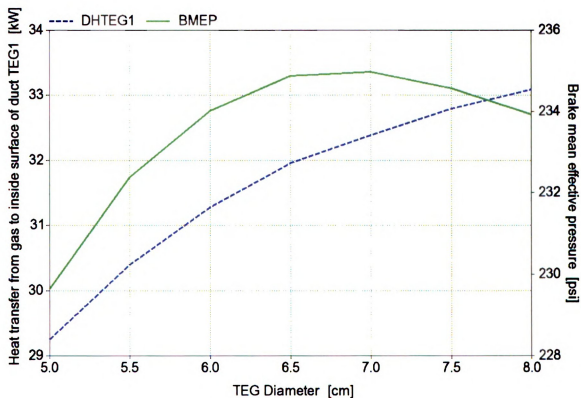


Figure 12: Effect of TEG effective diameter – single cylinder case

As TEG diameter is reduced, the BMEP does not change substantially until the diameter is less than 6.5 centimeters. This general behavior is expected, since reductions in the effective flow area of the engine exhaust system eventually lead to a significant restriction of the exhaust gas flow and an accompanying increase in the engine pumping work. The figure also shows that DHTEG1 increases with larger cross-section diameters. This follows from the concomitant increase in interior surface area within the TEG available for heat transfer from the exhaust gases. Although the heat transfer coefficient also increases as diameter is decreased because of the associated increase in gas velocities, the dependence of the overall heat transfer in the TEG on surface area proves to be the dominant factor.

Based on these results, a diameter of 6.5 cm was chosen for the single cylinder case. Although larger diameters would increase the value of DHTEG1, the average velocities through the TEG would decrease substantially, adversely affecting the performance of the turbocharger turbine located immediately downstream from the TEG duct. Therefore, the “optimum” TEG diameter was chosen to be the smallest value that does not diminish the engine output (BMEP) at the B-62 operating point. Phase II studies will further refine these design parameter tradeoffs by modeling the full turbocharger and EGR bypass systems at both part and full load conditions.

Similar TEG diameter optimization studies were carried out for the three and six cylinder configurations, resulting in diameters of 7.5 cm and 8.5 cm, respectively.

The other primary TEG design parameter is its axial length. As expected, the modeling results indicate a nearly linear increase in DHTEG1 for lengths ranging from 0.5 meters to 2.5 meters. Within this range, the BMEP was not significantly affected. A final value of 1.5 meters was chosen for all three configurations due to estimated packaging limits for the ISX engine. Again, Phase II studies will further define this parameter. In the current feasibility study, we want to focus on the number and overall integration of the TEG(s) within the engine's exhaust system.

### **3.1.6 Effects of Unsteady Flow Dynamics on TEG Heat Transfer**

It is important to note that the basic characteristics of the gas dynamics within the exhaust ducting, and the TEG duct in particular, are very different for the three configurations of interest, primarily because of the differing number of cylinders connected to the TEG. Each cylinder produces one exhaust “blowdown pulse” per engine cycle during the initial stages of the exhaust valve opening. Each of these pulses contain high pressure and temperature exhaust gases from the cylinder that will traverse each exhaust duct and be transmitted or reflected at duct transitions (e.g., changes in cross-sectional area). This in turn results in dynamic variations in the gas-side heat transfer coefficient. Figures 8, 9, and 10 illustrate this by showing the variation in the exhaust gas temperature, heat transfer coefficient, and gas velocity, respectively, in the TEG at its midpoint in length. The three curves in each figure are the results for the optimized geometries of the one, three, and six cylinder cases.

Figure 13 shows distinct peaks in the gas temperatures for each of the cylinder blowdown events for the single cylinder (one broad peak) and the six cylinder (six peaks) cases. The three cylinder case has three primary peaks and three secondary peaks of lesser amplitude. The secondary peaks represent reflections of the primary waves at the ambient exit boundary. The abscissa is the engine crankangle for cylinder 1 in which zero crankangle degrees represents the TDC (top dead center) piston position at the beginning of the expansion stroke for cylinder 1. For reference, the exhaust valve begins opening at 134 crank degrees.

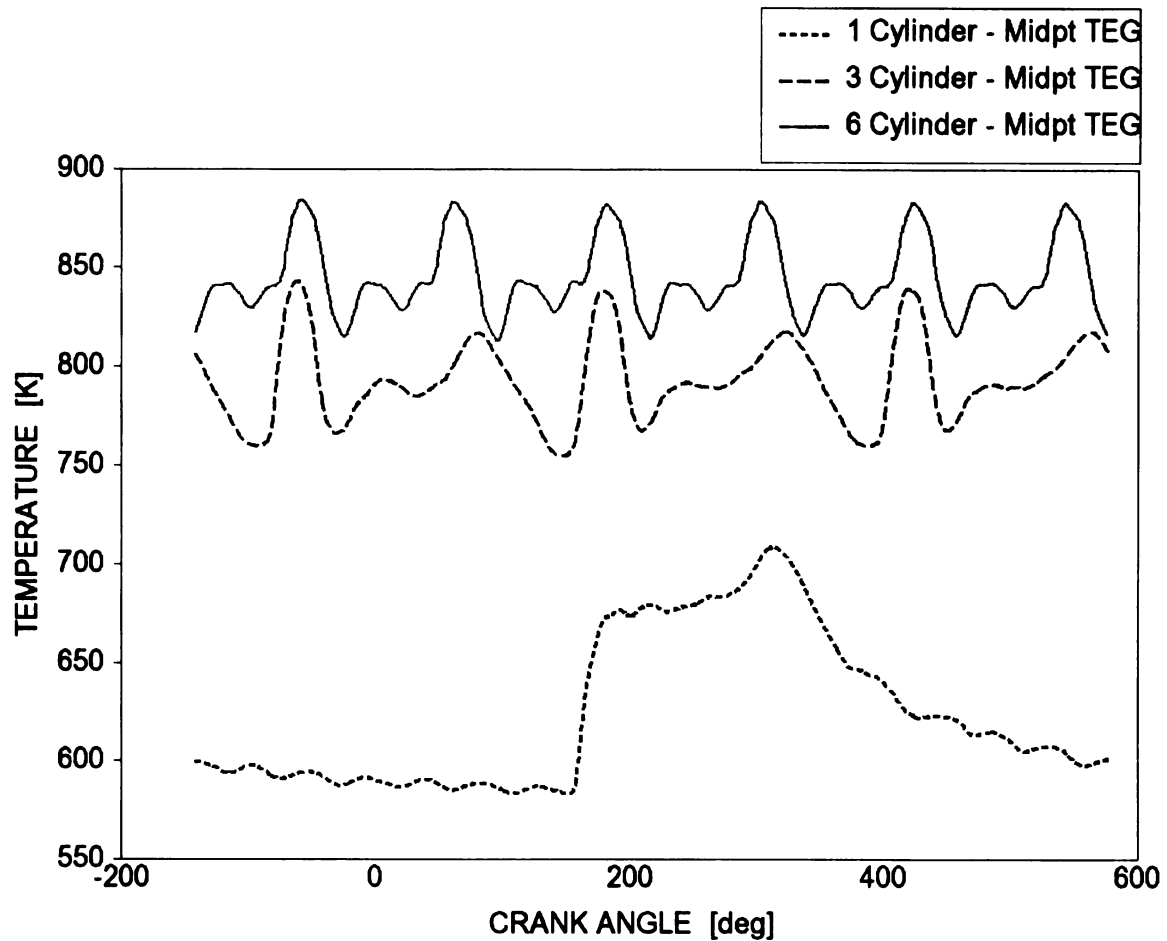


**Figure 13: Exhaust gas temperatures at TEG midpoint**

Figure 14 shows the corresponding heat fluxes to the TEG walls at its midpoint location. (A negative heat flux indicates heat transferred from the exhaust gases to the adjacent walls.) Again, distinct primary peaks are observed, depending on the number of cylinders “feeding” the TEG. The single cylinder case has the higher amplitude heat flux because of the higher gas velocities, shown in Figure 15. The higher velocities, in turn, are a result of the smaller cross-sectional area needed to expel the exhaust gases from a lesser number of cylinders.

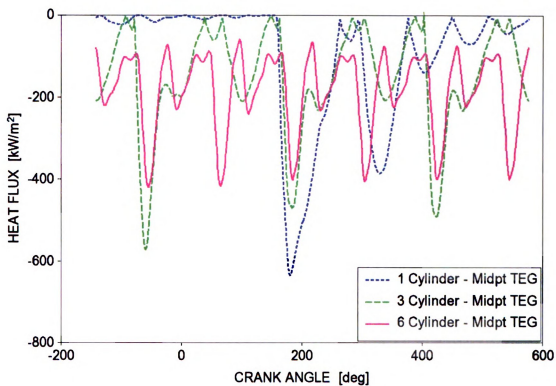


Figure 14: Heat flux at TEG midpoint

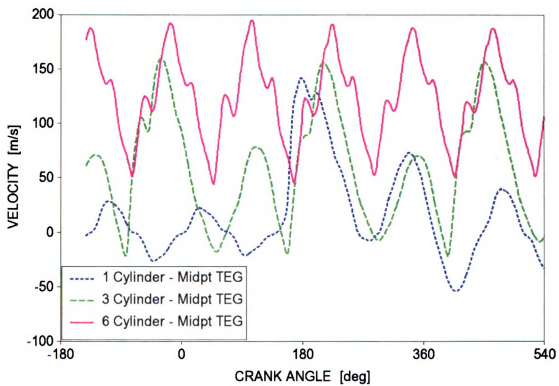


Figure 15: Gas velocities at TEG midpoint

### 3.1.7 Overall Results for Phase I

Table 4 summarizes the overall results of this Phase I analytical study of the potential viability and benefits of the application of TEG technology to the ISX engine.

All results are for the B-62 operating point. The second column displays the resulting value of DHTEG1, the average heat transfer rate from the exhaust gases to the walls of the single TEG in kW, for the one, three, and six cylinder configurations. The third column breaks this number down to a per cylinder value. The final column gives the amount of energy transfer rate from the complete engine/TEG system in which there are a total of six, two, or one TEG, respectively, for each of the configurations.

**Table 4: WAVE heat transfer results for one, three, and six cylinders per TEG configurations**

<b>Configuration (Optimized Geometry)</b>	<b>TEG Energy Input Rate [kW]</b>	<b>Energy Input per Cylinder [kW/cylinder]</b>	<b>Total TEG Energy Input [kW/engine]</b>
One Cylinder per TEG	31.9	31.9	191.4
Three Cylinders per TEG	50.2	16.7	100.4
Six Cylinders per TEG	64.5	10.8	64.5

The overall results indicate that more energy is extracted per cylinder per engine cycle for the single cylinder configuration. This follows primarily from the fact that the total wetted gas-side surface heat transfer area of the TEG per cylinder is three and six times greater, respectively, than for the three and six cylinder configurations. Also, the lower frequency of exhaust “events” per engine cycle for the single cylinder case, allows the interior walls more time to cool off between pulses and, thereby, provide a larger average temperature gradient to “drive” the transfer of energy from the exhaust gases to the TEG structure. Table 5 shows the time-average wall and exhaust gas temperatures at the inlet and exit of the TEG for each configuration. Both temperature values increase as the number of cylinders feeding the TEG increases.

**Table 5: Average TEG gas and wall temperatures**

<b>Configuration</b>	<b>Wall Temp (TEG Inlet) [K]</b>	<b>Gas Temp (TEG Inlet) [K]</b>	<b>Wall Temp (TEG Outlet) [K]</b>	<b>Gas Temp (TEG Outlet) [K]</b>
One Cylinder per TEG	708	856	597	634
Three Cylinders per TEG	798	884	662	711
Six Cylinders per TEG	831	898	731	785

The result above is that one TEG unit per cylinder is more effective and preferred over the cases of one TEG per three or six cylinders. This result has profound implications for the development and testing of TEGs for application to internal combustion engines. Most importantly, a single cylinder test engine, rather than a multi-cylinder (three or six) engine, is all that is necessary in the first development and test phase of the TEG. This in turn substantially lowers the time and cost to fabricate the prototype TEG designs, as well as that of the associated testing. Moreover, the WAVE engine simulation can be used in conjunction with this hardware design and testing to further optimize the TEG for packaging, as well as function. Following tests on a single cylinder engine, WAVE can be calibrated to the experimental data and then used to project the TEG and engine performance on the full Cummins ISX six-cylinder engine.

### 3.1.8 Electrical Energy Utilization

The electrical systems and modeling team envisions the recovery of engine waste heat in large OTR trucks for the primary purpose of redirecting this energy to the vehicle's wheels. Recovery of waste heat and its immediate delivery to the vehicle wheels in effect turns this concept into a thermal power split hybrid. This is a micro hybrid to be precise.

The overall architecture of the thermal power split hybrid is shown as Figure 16.

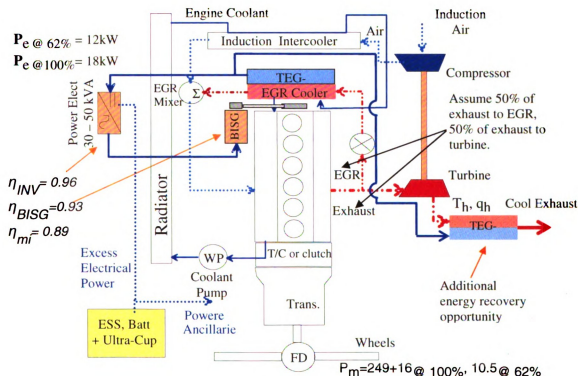


Figure 16: Architecture of the thermal power B-62 operating point

In the system of Figure 16, a fraction of the heat rejected via the engine exhaust will be returned to the engine induction port via an EGR loop. Opportunity for energy scavenging exists in the EGR loop because a conventional EGR system will incorporate an EGR cooler to cool the exhaust gas to near ambient conditions. Rather than reject this heat through the radiator, the presence of a thermoelectric generator, TEG, will use the

presence of a thermal gradient to convert a fraction of this rejected heat directly into electrical power as shown. The remainder of the engine-rejected heat is delivered in the conventional manner to the turbine side of the turbo charger and from there to the exhaust system.

The recovered waste heat from the EGR loop is matched to the hybrid drive system at a nominal potential of 144 VDC. At this voltage level two important attributes are realized: 1) it is economical using today's power electronics and electric machine technology to process up to 20 kW or more, and 2) the required number of total TEG couples at 144 V is less than if a 42 V nominal electrical distribution bus voltage is selected. The net effect of both benefits is that overall warranty is improved because fewer couples are series connected and moreover, the need for excessive parallel paths is minimized.

Electricity generated by the TE system is converted into mechanical work by the belt integrated starter/generator (BISG). The BISG will reduce the load on the engine and therefore improve efficiency of the overall powertrain. Some additional benefits of a BISG include providing a start/stop capability of the engine to reduce idling time and some degree of regenerative braking while the truck is coasting.

### 3.1.9 BSFC Calculation

Improvement of Brake Specific Fuel Consumption (BSFC) is the overall goal of this project. That being the case, a method of calculating the improvement was necessary.

BSFC is calculated as follows in Equation 3.1:

$$BSFC = \frac{Fuel\ Rate}{Power\ Output} = \frac{kg/hr}{kW} \quad (3.1)$$

As previously mentioned, the WAVE model fuel rate (kg of fuel per hour) was calibrated to match the Cummins test data. Since the fuel rate cannot change, the BSFC will improve (numerically lower) as the total power output increases. The calculation to determine the percent improvement in BSFC is:

$$\% \text{ imp. in BSFC} = \frac{Q_{TEG} \cdot N_{TEG} \cdot \eta_{TEG} \cdot \eta_{BISG} \cdot \eta_{INV}}{0.746 \cdot BHP} \times 100 \quad (3.2)$$

Where:

$Q_{TEG}$  = Gas side heat transfer to TEG duct wall (kW)

$N_{TEG}$  = Number of TEGs being evaluated

$\eta_{TEG}$  = Efficiency of TEG (Dependent on temperature gradient)

$\eta_{BISG}$  = Efficiency of Belt Integrated Starter Generator (96 %)

$\eta_{INV}$  = Efficiency of Inverter and Power Electronics (93 %)

$0.746 * BHP$  = Brake Horsepower converted to kW

(334.1 hp @ B-62 per Cummins data)

In the percent improvement in BSFC equation above, the numerator calculates the amount of additional power which is introduced to the engine belt drive from the thermoelectric and electrical drive systems. In Equation 3.2 the efficiency of the TEG was estimated based on the temperature gradient reported by each TEG configuration.

The TEG efficiencies used in the calculation were 9.1%, 11%, and 12.3% for the one, three, and six cylinders per TEG configurations respectively. The denominator of Equation 3.2 is the crankshaft power produced by the WAVE model. Therefore this equation yields the percentage of power increased over the crankshaft power output. As the BSFC is dictated by the total power in the system, this percentage directly translates to an improvement in BSFC.

A calculation for the improvement of BSFC was calculated using the values from Table 4 and the 334.1 horsepower from the Cummins test data (Table 3) and compiled in Table 6 below. The horsepower from the Cummins test data was used in the BSFC calculation rather than the WAVE reported horsepower. This was done in order to draw a better comparison between the three different TEG configurations.

**Table 6: BSFC percent improvement for three Phase I configurations**

<b>Configuration (Optimized Geometry)</b>	<b>TEG Energy Input Rate [kW]</b>	<b>BSFC Improvement [%]</b>
One Cylinder per TEG	191.4	6.2
Three Cylinders per TEG	100.4	4.0
Six Cylinders per TEG	64.5	2.8

### **3.1.10 Conclusions for Phase I**

The objective of this Phase I analytical study was to quantify the potential benefits of thermoelectric generator (TEG) design alternatives in converting waste exhaust heat from the Cummins ISX, 15 liter, 6-cylinder, diesel engine into electrical energy. The studies are carried out for engine operating conditions most representative of those for an on-road, eighteen-wheeled, Class 8 truck. To determine the maximum possible energy available for conversion, the TEG was located in the exhaust system immediately downstream from the engine's exhaust ports and manifold where it could serve as a possible replacement for the current engine's EGR (Exhaust Gas Recirculation) cooler. It was assumed that 100% of the exhaust gases pass through the TEG.

The study indicated several important results:

- 1) A greater amount of exhaust energy can be extracted through the TEG when each cylinder of the 6-cylinder engine has its own separate TEG passage, as opposed to alternate designs having three or six cylinders "feeding" a single TEG unit. Comparing the most practical designs of one versus three cylinders per TEG unit, simulation results for the B-62 (1500 rpm and 62% of full load) highway cruise operating point predict that the single cylinder configuration allows over 90% more energy extraction through the TEG unit per cylinder than the three-into-one design. For the full 6-cylinder ISX engine, this indicates that 191.4 total kilowatts of exhaust energy could be extracted from the exhaust gases and is, therefore, available for conversion into electrical energy. A significant consequence of this finding is that the next stage of TEG design, development, and testing can be carried out using a single cylinder engine test rig, as opposed to the full 15 liter, 6-

cylinder engine. This would lead to substantial cost and time savings as TEG prototypes would be one-sixth smaller and therefore require fewer P-N modules. Also, the WAVE engine simulation code can then be calibrated to the single cylinder test data and used to project the impact of each design iteration on the six-cylinder ISX engine.

- 2) Using liquid coolant, equivalent to that used in the engine cooling system (and assumed to be at a constant 325 degrees K), to cool the outer walls of the TEG results in average exhaust gas-side wall temperatures in the range of about 600 – 700 degrees K.

## **3.2 Phase II**

### **3.2.1 Expansion of Simplified Model**

The second phase of this study involves modeling the more realistic case of the full six-cylinder ISX engine with the TEG unit(s) fully integrated into the engine induction and exhaust systems, such that the engine exhaust gases divide between the TEG unit and the variable-geometry turbine. This configuration is similar to the actual ISX engine and is necessary to understanding the balance of the exhaust energy flow split between the TEG and the variable geometry turbocharger in order to meet the engine's power output, fuel consumption, and NOx emissions requirements. Figure 17 shows the new system model illustrating the manner in which the TEG now connects to one outlet of the exhaust manifold, while another exhaust outlet connects to the turbine inlet. Part of the experimental data supplied by Cummins detailed some of the intake/exhaust manifold geometry and was used where applicable. In the case that geometry data was not provided, the dimensions were approximated from pictures of the actual engine and intake/exhaust manifold volumes which were provided by Cummins.

### **3.2.2 New devices and sub-models**

On the left side of Figure 17, the cloud represents the intake air inlet which feeds the compressor side of the variable geometry turbocharger (VGT). The compressed air then passes through an intercooler before entering the intake manifold plenum. The cloud on the right-hand side of the figure represents the outlet of a 1m long exhaust pipe connected to the outlet of the turbocharger turbine. The heavy black line connecting the compressor and turbine represents the mechanical shaft linkage and is not a gas flow path. New control system elements shown in Figure 17 include control actuators for the EGR valve,

which controls the outlet flow of the TEG/EGR-Cooler, and the “rack position” of the variable geometry turbine, which controls the inlet area size of the turbine.

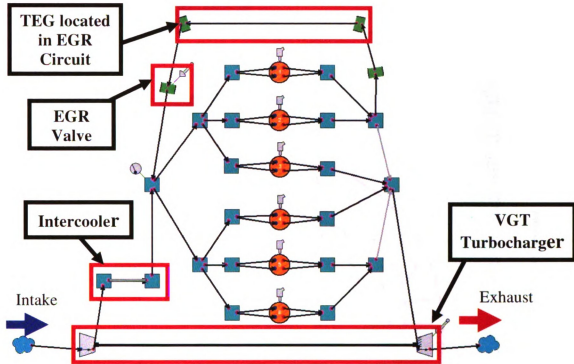


Figure 17: WAVE engine system layout of single TEG/EGR cooler configuration

### 3.2.3 Variable Geometry Turbocharger

The Cummins ISX engine utilizes a Variable Geometry Turbocharger (VGT). One piece of data which was not available from Cummins is the turbocharger maps for the VGT. This problem was overcome by using a combination of map data which was already in the WAVE code. The compressor map used was from a 10 L truck engine example which was scaled to mimic the required flow for the ISX engine, shown below in Figure 18. The map data was scaled by adjusting the diameter multiplier of the compressor or turbine which then multiplies the mass flow rate values listed in the map data.

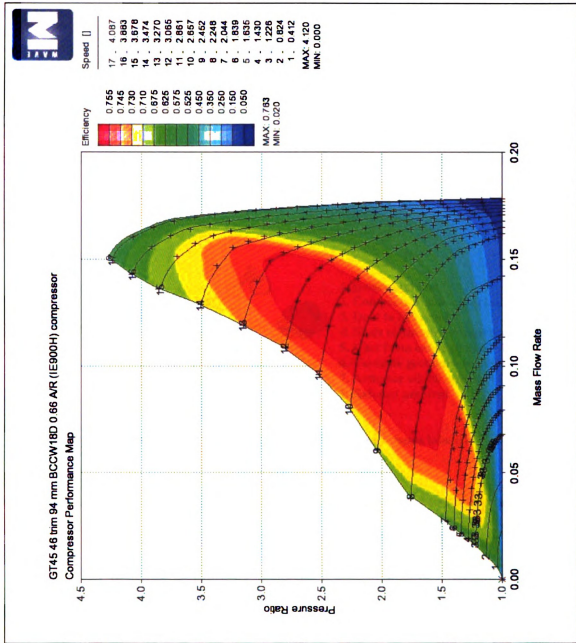
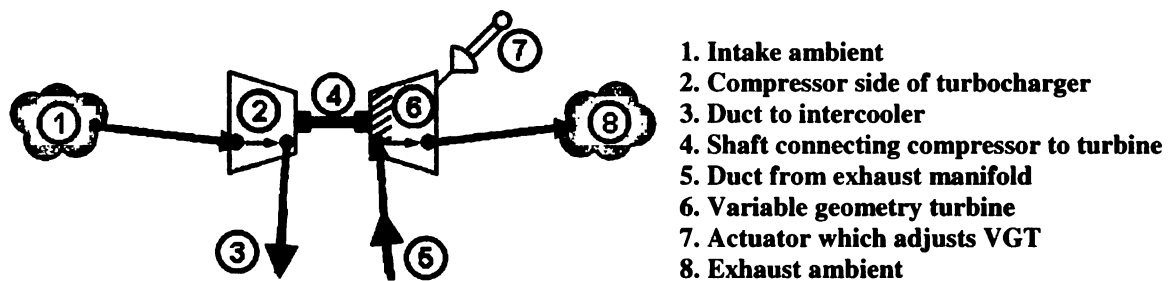


Figure 18: Compressor performance map

The VGT turbine maps (for each rack setting) came from another example engine which was a 4 L high-speed twin turbo diesel. The turbine maps are shown in the appendix. The “rack position” physically translates to adjusting the vanes or cross sectional area of the turbine to adjust performance. In the code the “rack position” determines which turbine

map is used in the calculations. If the “rack position” falls between maps the map data is interpolated from the adjacent “rack position” maps. These turbine maps were also scaled to represent performance similar to the actual turbocharger.

Figure 19 shows the WAVE icons which represent the VGT. Included are the intake/exhaust ambients, compressor/turbine, actuator to control the VGT and associated ducts and physical shaft connections.



**Figure 19: WAVE icons for the VGT with components labeled**

In real world applications a VGT system is most commonly used to reduce turbo-lag and also prevent damage caused by excessive boost pressure during operation. In this WAVE model the VGT is used to adjust the boost pressure automatically to match that supplied in the experimental data. This allows the code to adjust the turbocharger performance automatically to supply the boost necessary for the overall engine output to match that of the experimental data for each load point as various aspects of the model are modified. This turbocharger does not perform exactly like the physical device, but this is acceptable since no transient effects are being studied. If the model in the future were used to test transient effects, the turbocharger maps would need to be reevaluated.

### 3.2.4 Intercooler

Exact dimensions of the intercooler were not supplied by Cummins. However, inlet/outlet pressures and temperatures were supplied. Therefore an intercooler was copied from the 10 L truck example engine built into the WAVE code and the parameters were changed until the cooling and flow performance were approximately that of the experimental data. In WAVE the intercooler is treated as several small ducts which have ambient temperature air flowing over the outside approximating a heat exchanger. Figure 20 shows the WAVE icons for the intercooler with the components labeled. Newer versions of the WAVE code have a heat exchanger sub-model, which may provide a closer approximation of the experimental results if it should become necessary in the future.

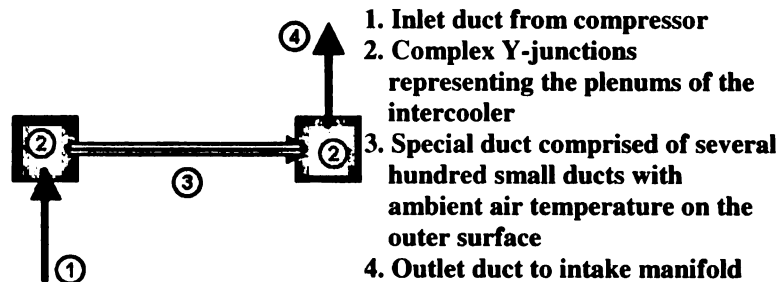


Figure 20: WAVE schematic of the intercooler

### 3.2.5 EGR Circuit

Exhaust gas recirculation (EGR) is used in most modern IC engines to meet NO<sub>x</sub> emission requirements. When exhaust gas is mixed with the fresh air entering an engine the peak temperature reached during combustion is reduced. This reduces engine efficiency but the lower temperature stops the formation of NO<sub>x</sub>. The EGR circuit consists of the ducting, TEG/EGR cooler and the valve required for the introduction of

exhaust gas into the intake manifold. The EGR circuit presented a similar challenge to that of the intercooler, in that there was little information provided on the dimensions of the EGR system. As in the case of the intercooler, experimental data was presented for the inlet/outlet pressures and temperatures of the EGR cooler. Some problems encountered were keeping the exhaust gas flowing in the correct direction and maintaining the correct EGR fraction in the intake charge. On the ISX engine the intake boost pressures can be great enough to reverse the EGR flow if the correct pressure gradient between the intake and exhaust manifolds is not maintained. With much trial and error, eventually a system was devised which utilized a single TEG duct acting as the EGR cooler and a valve located between the TEG/EGR cooler and the intake manifold. Figure 21 illustrates the EGR circuit and the associated components.

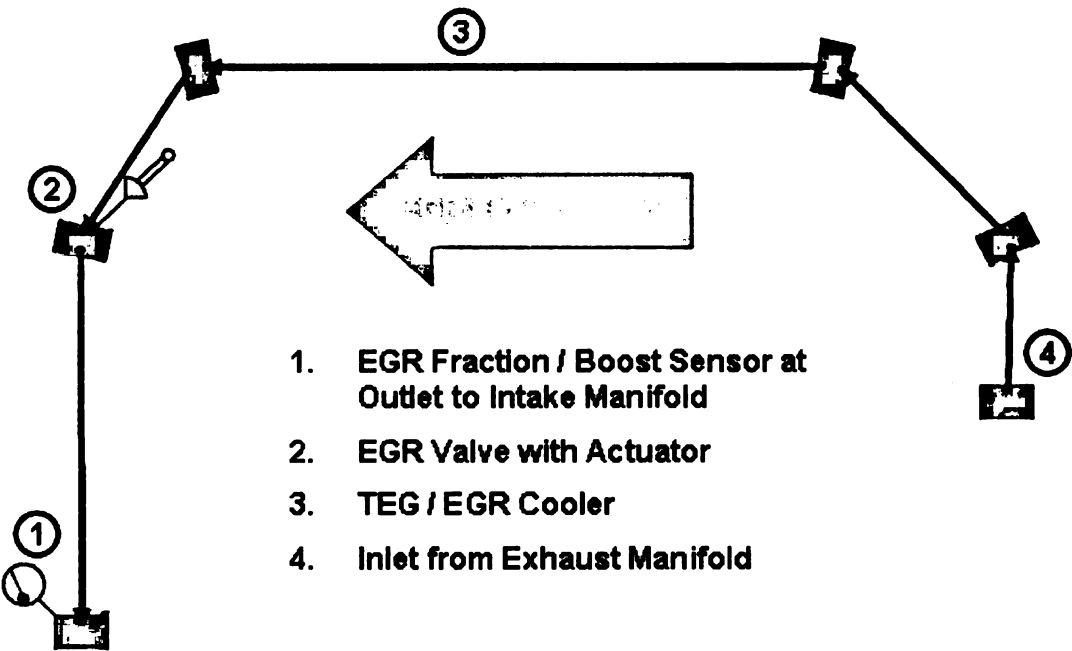


Figure 21: WAVE diagram of the EGR circuit with labels

At this stage the cooled exhaust gas is approximately 100 K higher than the experimental data. This is primarily because the TEG/EGR cooler was not modeled as a heat exchanger, as the intercooler had been. The thermoelectric material on the duct is acting somewhat like an insulator and prevents exhaust heat from escaping. It is believed that in actual operation the TEG will perform in this fashion. Even though the temperature is higher than it should be, the overall model engine performance is quite close to that of the experimental data and was therefore accepted as reasonable.

### **3.2.6 Control System**

Achieving an accurate simulation of this complex engine system presented several challenges. Most important, controlling the EGR fraction (i.e., the required fraction of the total intake gases that are exhaust gases circulated through the TEG/EGR cooler) and the VGT rack position, which determined the turbocharger boost pressure and correspondingly the specified engine power output, required use of the WAVE software feedback control system feature. The controller was given target EGR fraction values derived from test data which is shown in Table 3. By using this approach the software itself would adjust to changes elsewhere in the model automatically. The controller is a PID which has automatically calibrated gains. In order to calibrate the controller automatically, WAVE will move the actuator slightly and determine the response time of the sensor. In order to calibrate effectively, the auto-calibrate routine must be conducted several hundred times for each case in the model. The auto-calibration of this model can take over a day to complete.

### **3.2.7 Sensors and Actuators**

Sensors and actuators are two components which must be added to the model in order for the control system to function. The sensors consisted of an EGR fraction sensor and a pressure sensor which take their readings from where the ducts from the intercooler and EGR circuits join the intake manifold as shown as #1 in Figure 21. Since the EGR fraction of the intake air is commonly controlled by an EGR valve, an actuator was employed to control the diameter of an orifice between the intake manifold and the TEG/EGR cooler. The EGR valve actuator is shown in Figure 21 as #2. The other actuator used was for VGT rack position which controls the angle of the inlet vanes in the turbine. By adjusting the rack position the turbine wheel will speed up or slow down and therefore increase or decrease the amount of boost pressure created by the compressor. This VGT actuator is shown in Figure 3.2.2 as #7.

### 3.2.8 WAVE Model Validation

The WAVE code was used to simulate the baseline ISX production engine at each of the five operating points to validate model results against dynamometer data provided by Cummins engine. These model validation results are shown in Table 7 below. The major output parameters for all but one case match the Cummins data within 10%, which is considered acceptable for this type of modeling. Table 7 shows the correlation between the WAVE modeling predictions for brake torque (ft-lb), brake horsepower, airflow (kg/hr), EGR fraction, and compressor boost pressure (bar).

**Table 7: Comparison of Cummins test data to WAVE model results**

	A-25			A-100		
	Cummins	WAVE	%Diff	Cummins	WAVE	%Diff
<b>TORQBR</b>	472.2	485.2	2.8	1886.8	1879.8	-0.4
<b>BHP</b>	110.6	113.7	2.8	441.8	440.3	-0.3
<b>AIRKGH</b>	539.1	529.6	-1.8	1300.4	1305.8	0.4
<b>EGR</b>	0.265	0.274	3.4	0.171	0.171	0.3
<b>BOOST</b>	1.467	1.369	-6.6	3.069	3.083	0.5

	B-62			B-100		
	Cummins	WAVE	%Diff	Cummins	WAVE	%Diff
<b>TORQBR</b>	1170.2	1149.3	-1.8	1887.3	1752.6	-7.1
<b>BHP</b>	334.1	328.3	-1.7	538.8	500.6	-7.1
<b>AIRKGH</b>	1271.4	1226.9	-3.5	1729.4	1496.2	-13.5
<b>EGR</b>	0.214	0.218	1.8	0.201	0.201	0.1
<b>BOOST</b>	2.561	2.560	0.0	3.488	3.286	-5.8

	C-100		
	Cummins	WAVE	%Diff
<b>TORQBR</b>	1577.7	1461.3	-7.4
<b>BHP</b>	540.8	500.8	-7.4
<b>AIRKGH</b>	1862.0	1901.7	2.1
<b>EGR</b>	0.161	0.158	-2.2
<b>BOOST</b>	3.109	3.351	7.8

For the B-100 load point (1500 rpm/full load), the total airflow prediction is -13.5% different than the measured result. While this value is outside the +/- 10% range it is still considered to be adequate considering that the brake torque, which is dictated by airflow, is still in the range. Because the VGT rack was at its fully closed (max boost) position at this load point, it has been assumed that the airflow would match better if the actual turbocharger map data was used. These results provided some confidence in the overall modeling approach accuracy, allowing us to consider results for TEG output and therefore the BSFC improvement.

### **3.2.9 Results**

Once the model had been validated as being a good approximation of the physical engine, various parameters of the model can be examined. The inner and outer wall temperatures of the TEG are of particular interest. These values can be given to the material science engineers in charge of developing the thermoelectric material. Then they can use the temperature data to select an appropriate material and predict the thermoelectric efficiency, which is fraction of heat input energy that will be converted to electricity. Figure 22 below illustrates that the inner (T2) and outer (T3) wall temperatures reported by WAVE are calculated radially in the middle of each material thickness. The temperatures T2' and T3' are of interest to the TE materials group as these are the temperatures at the interfaces. The interface temperatures are important because these temperatures establish the thermal gradient which the TEG relies upon to function. The temperatures for T2 and T3 under EGR Cooler in Figure 22 are from the B-62 operating point. The temperatures are recorded axially at the inlet, midpoint, and outlet of the TEG duct.

Axial Pos	TEG Config	T2	T2'	T3	T3'
Outlet	6-1	731	727	524	342
Midpoint	6-1	781	777	546	338
Inlet	6-1	831	826	567	334
Outlet	EGR Cooler	461	460	391	329
Midpoint	EGR Cooler	560	558	437	329
Inlet	EGR Cooler	710	706	513	340

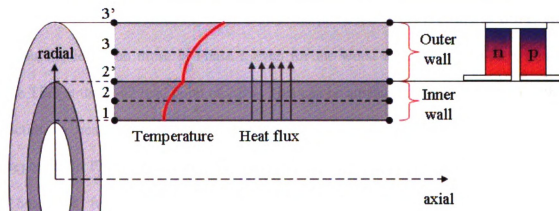


Figure 22: Diagram comparing wall temperatures for the single TEG/EGR cooler configuration at the B-62 operating point with the Phase I six cylinders per TEG configuration

The inner and outer wall temperatures of the TEG/EGR cooler duct for all five operating points are compiled below in Table 8.

Table 8: Inner and outer wall temperatures for single TEG/EGR cooler concept

Inner Wall Temperature(K)					
Axial Pos	A-25	A-100	B-62	B-100	C-100
Inlet	546	815	710	936	862
Midpoint	429	600	560	732	670
Outlet	375	472	461	571	513
Outer Wall Temperature(K)					
Axial Pos	A-25	A-100	B-62	B-100	C-100
Inlet	433	564	513	622	587
Midpoint	375	457	437	520	490
Outlet	350	397	391	445	417

### 3.2.10 BSFC Calculation for Single TEG/EGR Cooler

Utilizing the equation for the improvement in BSFC from Phase I, the percent improvement was calculated for all five operating points using the Phase II model, shown below in Table 9. At this point a TEG efficiency of 9.1% was adopted for the remaining BSFC calculations. It was assumed that this efficiency could be achieved for the typical temperature gradients reported by WAVE regardless of TEG location. The first conclusion that follows from the table is that the predicted improvements in BSFC are substantially less than those in Phase I, even for the worst case of six cylinders into a single TEG at the B-62 load point of 2.8%. This can be attributed in the calculation to the reduction in heat flux through the thermoelectric material and slightly lower crank horsepower. In Phase I all of the exhaust was flowing through the TEG, and as a result the heat flux for the B-62 load point was calculated to be 64.5 kW which is approximately twice the heat flux of Phase II.

**Table 9: BSFC percent improvement for single TEG/EGR cooler**

<b>Load Point</b>	<b>TEG Heat Transfer Rate (kW)</b>	<b>WAVE BHP</b>	<b>BSFC Improvement (%)</b>
<b>A-25</b>	14.64	113.65	1.4
<b>A-100</b>	39.83	440.27	1.0
<b>B-62</b>	32.34	328.28	1.1
<b>B-100</b>	53.28	500.59	1.2
<b>C-100</b>	47.63	500.84	1.0

However, one cannot make a direct comparison of the TEG output between that of Phase I and Phase II for two reasons. First, in Phase I the TEG received the full exhaust flow. In Phase II, for the B-62 load point, the TEG/EGR cooler has 20% of the exhaust flow diverted into the duct. Second, in Phase II the internal diameter of the TEG duct was

increased from 6.5 cm to 8.5 cm. This was done to approximate the cross-sectional flow area of the physical EGR cooler. This resulted in an increase of internal surface area of the TEG/EGR cooler by approximately 30% which is used in the calculation of the heat flux.

### **3.2.11 Summary of Phase II**

In Phase II a more realistic model has been created in WAVE which includes many features which were omitted in the Phase I efforts. The TEG has been placed in the EGR circuit and no longer receives the full exhaust flow. A variable geometry turbocharger was added to the model as well as an intercooler to lower the intake air temperature. A control system was implemented to adjust the EGR valve automatically and the VGT rack position during simulation. The model was validated to the Cummins test data and was accepted as providing a reasonable approximation of the physical ISX engine. Data was collected from the model including TEG wall temperatures for use by the thermoelectric development group. An estimated BSFC percent improvement was calculated for all five operating points and ranged from 1.0 to 1.4% improvement.

### **3.3 Phase III**

#### **3.3.1 TEG Placement Concepts**

The WAVE engine system modeling has been expanded to explore different TEG placement opportunities with emphasis on obtaining higher temperature gradients across the TEG and thereby achieve further improvements in BSFC. Several placement possibilities were explored including a secondary TEG after the turbocharger, a TEG on each exhaust port similar to the Phase I study, and the integration of an additional heat exchanger into the EGR circuit after the TEG. A new strategy in calculating BSFC is developed using an improved baseline model.

#### **3.3.2 Dual TEG**

As a first attempt to achieve a higher percent improvement in BSFC, an additional TEG was included in the exhaust stream after the turbocharger as shown in Figure 23 below. This concept is based upon the relationship of inner surface area to TEG output discussed in Phase I. In order to obtain the maximum surface area possible, the lengths of both TEGs were also increased from the 150 cm (in Phase I and the initial Phase 2 results above) to 200 cm. Increasing the length of the TEG/EGR cooler by 50 cm increased the inner surface area by 33% which will subsequently increase the amount of heat transfer into the duct wall.

The second TEG was simply a copy of the TEG/EGR cooler from Phase II, which was attached to the outlet of the turbine in place of the 100 cm exhaust duct leading to the exhaust ambient. The only modification to any of the second TEG's parameters was increasing the inner diameter from 8.5 to 10.16 cm to match the duct it is replacing. The secondary TEG has an inner surface area 20% larger than the single TEG/EGR cooler. The combination of the two TEGs increases the total inner surface area by 193% over that of the single TEG/EGR cooler configuration.

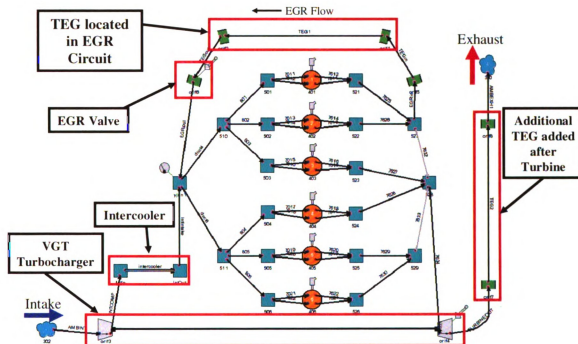


Figure 23: WAVE diagram for the dual TEG configuration

The percent improvement in all five points was again calculated and compiled below in Table 10. Here we see that the total TEG energy input rate is more than double that of the single TEG/EGR cooler studied in Phase II. Also the percent improvement in BSFC is nearly the 2.8% which was predicted in Phase I for the B-62 load point.

**Table 10: BSFC percent improvement for dual TEG configuration**

<b>Load Point</b>	<b>Total TEG Energy Input Rate (kW)</b>	<b>BHP</b>	<b>BSFC Improvement (%)</b>
<b>A-25</b>	37.03	114.28	3.5
<b>A-100</b>	98.01	444.76	2.4
<b>B-62</b>	74.85	329.82	2.5
<b>B-100</b>	127.34	510.51	2.7
<b>C-100</b>	117.83	516.59	2.5

By extracting exhaust heat downstream from the turbine there were no negative effects on engine power output. All of the operating points reported an increase in BHP as well as greatly increasing the total heat flux in the TEGs.

Figure 24 below compares the BSFC percent improvement for the dual TEG and single TEG/EGR cooler configurations for all five operating points. By adding the secondary TEG the total surface area was increased more than three times over the single TEG/EGR cooler. This larger surface area increased the total TEG energy input rate by 130-150%. Comparing the two configurations the dual TEG configuration shows more than double the percent improvement in BSFC than the single TEG/EGR cooler for all operating points. The higher crankshaft horsepower for all five operating points also contributed to the increase in BSFC percent improvement.

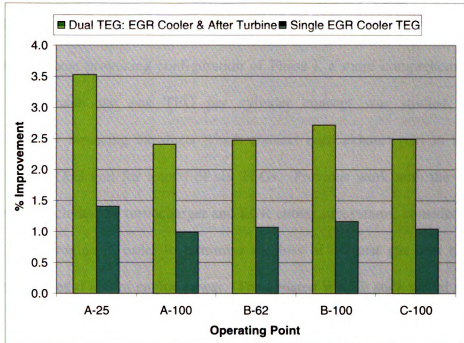


**Figure 24: BSFC percent improvement comparison for single TEG/EGR cooler and the dual TEG configuration**

### 3.3.3 TEG on Each Exhaust Port

Similar to the most promising configuration of Phase I, a more comprehensive engine system model with the one TEG per cylinder concept was studied. This was accomplished by replacing the ducts which connect each exhaust port to the exhaust plenum with a TEG unit for a total of six TEGs. Previous work with the full engine model, which includes the turbocharger and EGR cooler subsystems, considered one and two TEGs per engine in order to minimize the loss of exhaust gas heat energy and, therefore, a potential loss of engine power. The updated WAVE stick model is shown in Figure 25. Each TEG duct is basically a copy of the TEGs that were modeled in previous work.

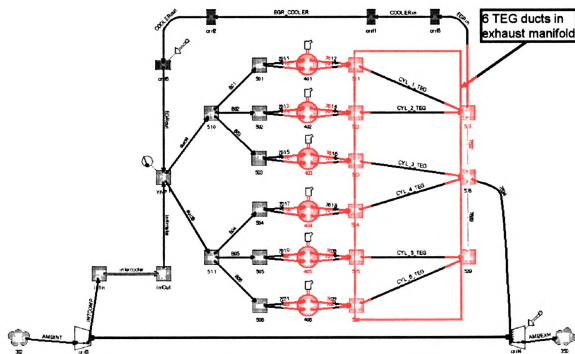


Figure 25: WAVE stick diagram showing the 6 TEGs in the exhaust manifold

For each speed/load point, if engine power decreased as a result of reductions in turbine inlet energy, attempts were made to recover the loss through changes in turbocharger geometry, specifically the multipliers for compressor and turbine diameters. These multipliers scale the mass flow rates from the turbo map data and therefore effectively scale the turbochargers' performance.

Each of the TEGs attached to the exhaust ports is a copy of the TEG/EGR cooler from the previous iteration of the model. The inner diameter and the length of the TEG duct were the same as the ducts which were replaced. It should be noted at this time that the TEG/EGR cooler duct is still in place even though it is labeled as EGR\_COOLER in Figure 25. The heat transferred to the TEG/EGR cooler was not included in the following calculations. This was done in order to obtain a better understanding of how effectively the six TEGs perform in a configuration similar to Phase I.

Once the TEG ducts were in place, a parametric study was undertaken to determine the effect of the TEG duct lengths on the engine performance. The lengths of the ducts were varied from 10cm to 150cm with calculations being performed at 10cm increments. The engine horsepower output is compared with the TEG duct lengths in Figure 26. At the initial length of 10cm, the horsepower output is essentially the same as the previous model, which was operating at the power levels provided by the Cummins test data. As the TEG duct length is increased, the horsepower output of the engine decreases, except for the A-25 load point of lowest engine speed and load. For the most important B-62 point, which best represents highway cruise conditions, there is no loss in BHP until TEG lengths are greater than 30 cm.

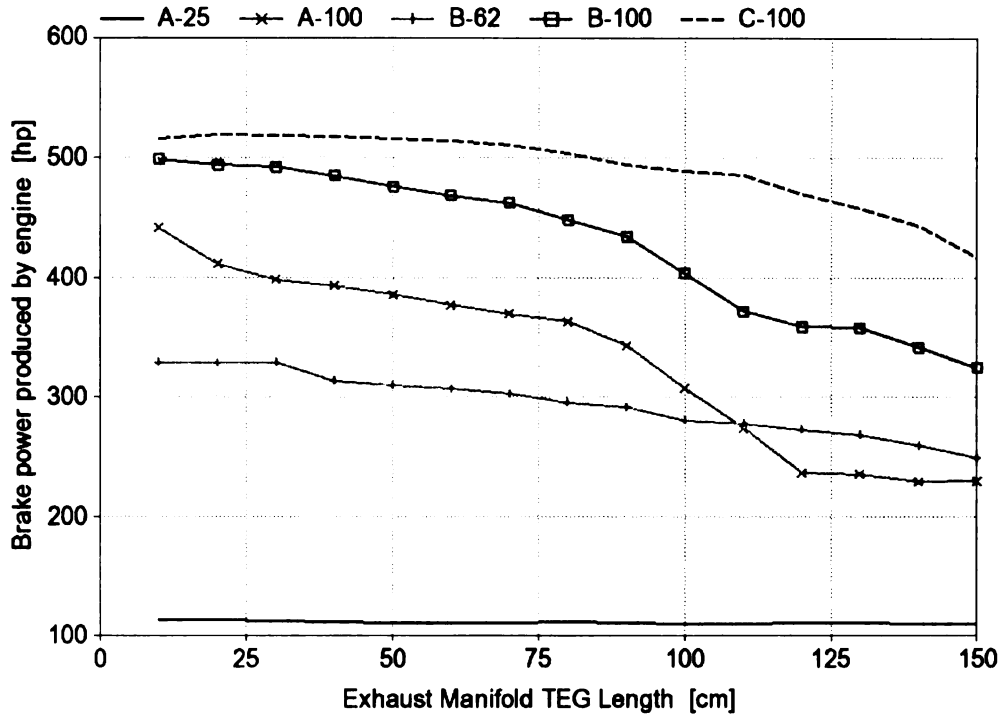


Figure 26: Plot of engine horsepower vs. TEG length for all 5 operating points

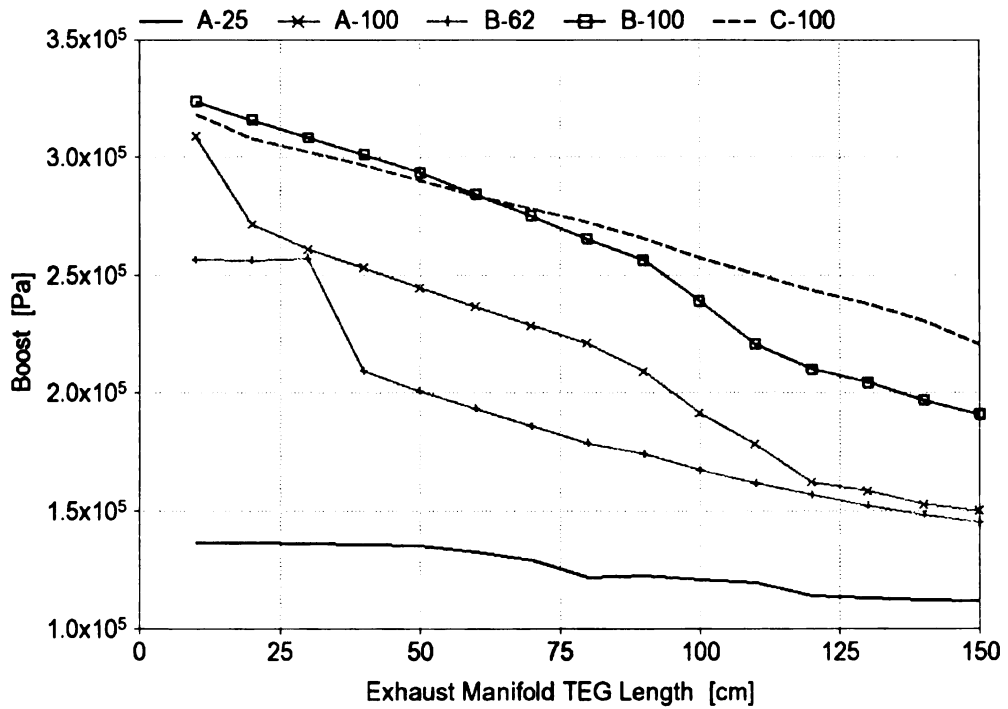


Figure 27: Plot of total TEG heat transfer vs. TEG length for all 5 operating points

Figure 27 shows the corresponding total heat flux produced by the 6 TEGs versus the TEG duct lengths. As seen in previous Phase I and Phase II studies, the heat flux is a strong, generally increasing, function of the TEG duct length. The exception to this trend is the load point A-100 at TEG lengths greater than 90 cm. This drop in TEG heat transfer can be attributed to the significant drop in engine power output.

While the heat transfer at the longer lengths is increased significantly, the engine performance depicted in Figure 27 decreases significantly. These results represent the best possible engine output achievable by the aforementioned attempts to re-optimize turbocharger turbine parameters.

It was determined that BHP losses for TEG lengths greater than 30 centimeters would be unacceptable by the manufacturer. Therefore, calculations were conducted at the length of 30cm to determine if there is potential for improvement in BSFC. Table 11 shows the results of the BSFC calculation. The highest improvement was 2.7% better than that of the base engine itself. The BSFC is dependent on the horsepower produced by the engine and when the fueling rate is held fixed, the BSFC will fluctuate with the engine power output.

**Table 11: BSFC percent improvement for 30cm TEG duct length (un-optimized)**

<b>Load Point</b>	<b>Total heat flux in TEGs (kW)</b>	<b>Brake Horsepower</b>	<b>BSFC Improvement (%)</b>
<b>A-25</b>	20.27	112.51	2.7
<b>A-100</b>	64.31	398.24	2.4
<b>B-62</b>	39.67	329.19	1.8
<b>B-100</b>	67.99	491.93	2.0
<b>C-100</b>	65.00	518.56	1.8

The horsepower output of the engine was down by over 10% for the 1230rpm (A-100) and 1500rpm (B-100) cases. The data in Table 11 above was compiled without changing the compressor and turbine multipliers which were set to 1.0 and 1.5 respectively. It appears that the engine model is operating quite efficiently at its current configuration for this fuel rate. Therefore, it does not appear to be possible to increase the power level further without increasing the fuel consumption. It is then concluded that while the pre-turbo exhaust manifold area is a good source of high temperatures and energy to drive a TEG, this energy cannot be extracted in large quantity without negatively impacting the overall engine performance.

### **3.3.4 TEG / EGR Cooler and Dual TEG Concepts with Heat Exchangers**

As the studies progressed, discussions with thermoelectric experts suggested that the TEG material acts more like an insulator than previously thought. Therefore, when used as a replacement for the EGR cooler, the TEG does not lower the EGR temperature as much as the original cooler would have. In many cases the EGR was more than 100 K higher than the Cummins test data. Since such a high EGR fraction is required to meet NO<sub>x</sub> emissions requirements, this was found to impact the overall performance of the engine negatively because the hotter EGR was heating the intake air charge and therefore reducing the power output of the engine. A simple solution to this was to integrate a small heat exchanger into the EGR circuit after the TEG to reduce the temperature of the EGR before being introduced to the intake manifold. This is somewhat counter to the original goal of eliminating the EGR cooler completely and replacing with a TEG. However, the performance increase of the engine power and therefore improving BSFC more than outweighs the cost and complexity of the additional components.



transfer and friction coefficients of the ducts are automatically varied to match the temperature and pressure drops between the inlet and outlet complex Y-junctions.

**Table 12: BSFC percent improvement: Single TEG/EGR cooler with and without heat exchanger**

<b>Load Point</b>	<b>TEG Energy Input Rate (kW)</b>	<b>BHP</b>	<b>BSFC Improvement (%)</b>
<b>Phase II Single TEG / EGR Cooler (No Heat Exchanger)</b>			
<b>A-25</b>	14.64	113.65	1.4
<b>A-100</b>	39.83	440.27	1.0
<b>B-62</b>	32.34	328.28	1.1
<b>B-100</b>	53.28	500.59	1.2
<b>C-100</b>	47.63	500.84	1.0
<b>Single TEG / EGR Cooler with Heat Exchanger</b>			
<b>A-25</b>	14.64	114.86	1.4
<b>A-100</b>	42.80	431.44	1.1
<b>B-62</b>	30.00	332.33	1.0
<b>B-100</b>	49.87	522.45	1.0
<b>C-100</b>	42.27	519.27	0.9

Table 3.3.3 makes a comparison between the single TEG/EGR cooler from Phase II and the modified version with the heat exchanger. In almost all cases the addition of the heat exchanger reduced the TEG energy input rate while increasing the BHP of the model. As shown in the table the addition of the heat exchanger did not improve the BSFC. The only exception was for the A-100 case. The A-100 operating point exhibited a total net power loss (crankshaft BHP + TEG power) of 6.45 kW. However, the BSFC percent improvement calculation reported an increase of 0.1% which is impossible according to the definition of BSFC. This discrepancy is explored further in the next section.



operating point. This is a bit contradictory because the engine horsepower output has increased in all but the A-100 operating point. This implies that there is a problem with the BSFC improvement calculation. Each kW gained in the TEG input energy rate will contribute about 0.1 kW to improving the BSFC. On the other hand, each horsepower which is gained in the model output is adding 0.75 kW to the BSFC. Therefore it can be concluded that crankshaft BHP has a greater effect on BSFC than the power generated via the TEG system. Any decrease in crankshaft BHP must be less than the additional power introduced by the TEG system for the BSFC to improve. This leads to the next section where the BSFC calculation is reevaluated.

**Table 13: BSFC percent improvement: Dual TEG with and without heat exchanger**

<b>Load Point</b>	<b>TEG Energy Input Rate (kW)</b>	<b>BHP</b>	<b>BSFC Improvement (%)</b>
<b>Dual TEG without Heat Exchanger</b>			
<b>A-25</b>	37.03	114.28	3.5
<b>A-100</b>	98.01	444.76	2.4
<b>B-62</b>	74.85	329.82	2.5
<b>B-100</b>	127.34	510.51	2.7
<b>C-100</b>	117.83	516.59	2.5
<b>Dual TEG with Heat Exchanger</b>			
<b>A-25</b>	35.26	114.89	3.3
<b>A-100</b>	103.00	434.31	2.6
<b>B-62</b>	67.76	334.72	2.2
<b>B-100</b>	111.68	522.76	2.3
<b>C-100</b>	113.31	521.23	2.4

### 3.3.5 Advanced BSFC Calculation

As the WAVE studies progressed, the BSFC Improvement calculation was found to be inadequate. While the earlier calculation (Equation 3.2) proved sufficient for the Phase I studies, it lacked the ability to compensate for power increases and decreases in the WAVE model. The revised calculation is shown below as Equation 3.3. The primary change made between the old and new equations is the ability to specify a baseline power number to serve as a point of reference. By implementing this we are able to compensate for situations where the WAVE model engine power output increases or decreases due to changes in TEG geometry and placement.

$$BSFC\ IMP.(\%) = \frac{Power_{Total} - Power_{Base}}{Power_{Base}} \times 100$$
$$Power_{Total} = Q_{TEG} \times \eta_{TEG} \times \eta_{BISG} \times \eta_{INV} + Power_{WAVE} \quad (3.3)$$

With the use of the new calculation it was decided to revisit the dual TEG study of Section 3.3.1.1 to observe the change on the BSFC Improvement numbers.

The single TEG/EGR cooler WAVE model was used as the baseline for this calculation. The single TEG/EGR cooler model was considered to be the most accurate model of the actual ISX engine created to date. The results of the calculation are shown in Table 14 below. It should be noted that the WAVE Power and the TEG heat flux are the same as

previously reported. The only change has been the inclusion of a baseline for comparison purposes. Results of the new calculation are compared to the previous results in Table 14.

**Table 14: Results of the new BSFC percent improvement calculation for the dual TEG study**

<b>Load Point</b>	<b>Total heat flux in TEGs (kW)</b>	<b>WAVE Power (kW)</b>	<b>Single TEG/EGR Cooler Baseline (kW)</b>	<b>BSFC Improvement (%)</b>
<b>A-25</b>	37.03	85.22	84.75	4.1
<b>A-100</b>	98.01	331.66	328.31	3.4
<b>B-62</b>	74.85	245.95	244.80	3.0
<b>B-100</b>	127.34	380.69	373.29	4.8
<b>C-100</b>	117.83	385.22	373.48	5.7

As shown in Figure 30, the BSFC percent improvement for the dual TEG case is actually better than previously reported. This is due to the fact that the WAVE engine power output actually increased over that of the baseline single TEG/EGR cooler model. Now it can be seen that there is a measurable improvement in BSFC in all cases, and in the case of C-100 it more than doubles the previous value.

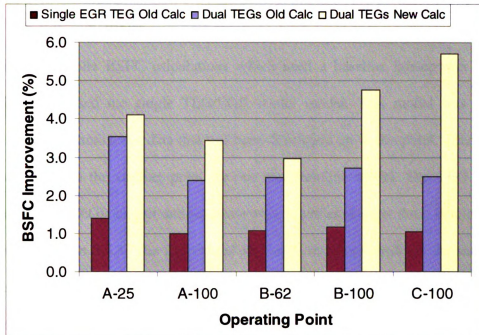


**Figure 30: Comparison of the results of the new BSFC percent improvement calculation to the previous calculations**

These results illustrated the need for a baseline model which can serve as a benchmark for model power output that does not include a TEG anywhere in the system. The next section covers this new baseline model that was developed.

### 3.3.6 New Baseline Model

Up until now all the BSFC calculations which used a baseline horsepower level for comparison had used the single TEG/EGR cooler model. This model was the most accurate to the Cummins test data that had been developed up to this point. Therefore this model was used as the starting point for our new baseline model. The TEG duct was removed from the EGR circuit and replaced with a heat exchanger duct, similar to what was used in Section 3.3.4. The function of the heat exchanger model is the same as the previous attempts, but in this case the duct used an inner diameter of 8.5 cm and a length of 150 cm. Figure 31 below shows the WAVE stick diagram of the baseline model.

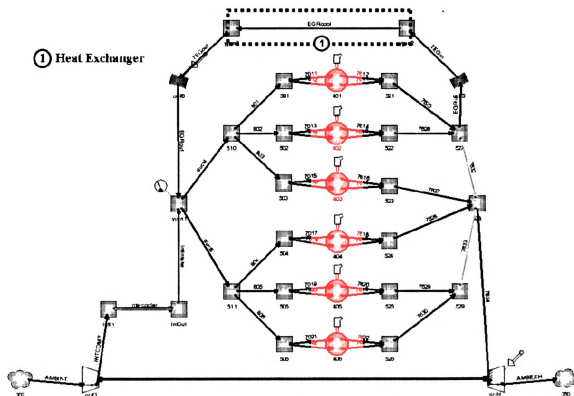


Figure 31: WAVE diagram of baseline model with heat exchanger replacing TEG

Great lengths were taken to ensure that this model mimics the performance of the Cummins ISX engine. Nearly every parameter that was supplied in the Cummins test data was compared to the baseline model. The percent difference of this comparison has been compiled into Table 15 below. The percent difference listed in Table 15 shows how close the baseline WAVE model is to the Cummins test data. If the percent difference is greater than 10% then the cell is colored red or blue depending on if the value is greater or less than  $\pm 10\%$ . The bulk of the values out of the  $\pm 10\%$  range are related to the EGR valve and cooler. It will be very difficult to get all of the temperatures and pressures to match exactly for this type of system, especially since little is known about the exact dimensions of the EGR circuit.

**Table 15: Comparison of percent difference between Cummins test data and baseline WAVE model**

Load Point	C-100	B-100	B-62	A-100	A-25
EngSpd	-0.02	0.05	0.05	-2.42	-2.43
EngTorq	-3.93	-3.08	-2.38	-3.42	3.99
Fuel Rate	0.01	0.01	0.01	0.01	0.02
Turbine Inlet Temp	-1.32	-1.49	-3.52	0.09	-8.76
EGR CLR Gas Out Temp	<b>-13.12</b>	<b>-13.54</b>	<b>-11.64</b>	<b>-11.65</b>	<b>-10.58</b>
A:F Dry	2.04	-4.01	-2.41	-4.75	5.09
Power (HP)	-3.94	-3.03	-2.33	-3.40	4.00
BMEP	-3.83	-2.98	-2.28	-3.33	4.09
PAM CMP In Temp	0.03	0.01	0.07	-0.01	-0.31
CMP In Press	1.73	1.65	0.92	0.97	0.22
PAM Air Flow	0.43	-5.52	-3.96	-6.18	3.49
PAM CMP Eff	<b>-11.89</b>	1.73	1.75	1.07	7.96
PAM COT	3.15	-4.86	-3.34	-4.88	-2.16
PAM CMP Out Press	-2.40	<b>-10.51</b>	<b>-7.23</b>	<b>-11.34</b>	-1.87
CAC Inlet Temp	-5.57	<b>-12.40</b>	-9.75	<b>-12.17</b>	-5.62
CAC Outlet Temp	-6.37	-6.03	-2.93	-4.14	-1.79
CAC Outlet Press	-5.97	<b>-13.01</b>	-9.69	<b>-13.30</b>	-3.53
Exh Prt #1 Temp	0.91	4.05	0.88	7.06	-4.30
Exh Prt #2 Temp	2.94	5.81	1.62	9.25	-4.38
Exh Prt #3 Temp	4.40	6.13	2.94	<b>11.16</b>	-4.10
Exh Prt #4 Temp	3.71	5.46	0.67	9.72	-5.40
Exh Prt #5 Temp	3.37	4.65	1.39	9.29	-5.39
Exh Prt #6 Temp	3.65	4.52	1.06	8.83	-3.54
PAM TinT	-2.29	-2.41	-4.30	-0.96	-9.32
PAM TinP	<b>30.91</b>	5.38	3.46	-6.21	-7.35
PAM ToutT	-2.76	1.25	-1.49	3.58	-7.50
PAM ToutP	<b>-18.67</b>	<b>-16.17</b>	<b>-10.33</b>	<b>-12.27</b>	-3.51
PAM TRB Eff	<b>-15.50</b>	<b>-21.78</b>	<b>-19.23</b>	<b>-15.08</b>	<b>16.46</b>
EGR Valve In Press	<b>38.48</b>	<b>11.13</b>	8.77	-1.95	-4.87
EGR Valve In Temp	<b>-13.11</b>	<b>-12.98</b>	<b>-11.16</b>	<b>-10.41</b>	<b>-10.79</b>
EGR Valve Out Press	-7.17	<b>-14.91</b>	<b>-12.37</b>	<b>-15.72</b>	-9.54
EGR Valve Out Temp	<b>-13.34</b>	<b>-12.70</b>	<b>-11.13</b>	<b>-10.99</b>	<b>-10.90</b>
EGR CLR Gas In Temp	<b>-21.28</b>	<b>-18.04</b>	<b>-17.94</b>	<b>-18.03</b>	<b>-13.32</b>
EGR CLR Gas In Press	<b>32.60</b>	5.95	2.95	-6.18	<b>-10.26</b>
EGR CLR Gas Out Temp	<b>-13.12</b>	<b>-13.54</b>	<b>-11.64</b>	<b>-11.65</b>	<b>-10.58</b>
EGR CLR Gas Out Press	<b>38.32</b>	<b>11.11</b>	8.74	-1.95	-4.75
EGR Cooler Eff	2.76	4.03	3.36	3.40	1.90
EGR MASS FLOW	-5.36	-8.01	-6.33	-6.46	7.57
EGR Fraction	-5.61	-2.55	-1.91	-0.49	2.34
Intake Manifold Press (Abs)	-5.16	<b>-12.23</b>	<b>-10.35</b>	<b>-12.88</b>	-6.47

Considering how well the data matches, this baseline model is accepted as a good representation of the production Cummins ISX engine. The baseline model power output which will be used in the BSFC calculations is listed below in Table 16.

**Table 16: Baseline engine model power output listed for each load point compared to Cummins test data**

<b>Load Point</b>	<b>Cummins Test Data (hp)</b>	<b>Baseline Model (hp)</b>	<b>Difference (%)</b>
<b>A-25</b>	110.57	114.99	4.00
<b>A-100</b>	441.78	426.78	-3.40
<b>B-62</b>	334.06	326.28	-2.33
<b>B-100</b>	538.77	522.46	-3.03
<b>C-100</b>	540.79	519.50	-3.94

The baseline model power levels are within 5% for all five operating points. For the B-100 and C-100 operating points, the horsepower levels of the baseline model are approximately 20 horsepower higher than the single TEG/EGR cooler model. It was decided to implement this baseline model for the BSFC calculations rather than use the Cummins test data because the WAVE model will not be able to exactly duplicate the performance of the physical engine. By using another WAVE model as the baseline, the comparisons drawn will be more consistent.

### **3.3.7 Updated BSFC Calculations for All Concepts**

Now that there exists a reasonable baseline model without a TEG, the BSFC percent improvement can be recalculated using the new equation. These percent improvements are listed below in Table 17 along with the percent difference between the baseline model and each concept's horsepower.

Table 17: Updated BSFC percent improvement for all concepts

Load Point	TEG Energy Input Rate (kW)	WAVE BHP	BHP Difference from Baseline (%)	BSFC Improvement Old Calc. (%)	BSFC Improvement New Calc. (%)
<b>Single TEG / EGR Cooler without Heat Exchanger</b>					
<b>A-25</b>	14.64	113.65	-1.17	1.4	0.2
<b>A-100</b>	39.83	440.27	3.16	1.0	4.2
<b>B-62</b>	32.34	328.28	0.61	1.1	1.7
<b>B-100</b>	53.28	500.59	-4.18	1.2	-3.1
<b>C-100</b>	47.63	500.84	-3.59	1.0	-2.6
<b>Single TEG / EGR Cooler with Heat Exchanger</b>					
<b>A-25</b>	14.64	114.86	-0.11	1.4	1.3
<b>A-100</b>	42.80	431.44	1.09	1.1	2.2
<b>B-62</b>	30.00	332.33	1.85	1.0	2.9
<b>B-100</b>	49.87	522.45	0.00	1.0	1.0
<b>C-100</b>	42.27	519.27	-0.04	0.9	0.8
<b>Dual TEG without Heat Exchanger</b>					
<b>A-25</b>	37.03	114.28	-0.62	3.5	2.9
<b>A-100</b>	98.01	444.76	4.21	2.4	6.7
<b>B-62</b>	74.85	329.82	1.09	2.5	3.6
<b>B-100</b>	127.34	510.51	-2.29	2.7	0.4
<b>C-100</b>	117.83	516.59	-0.56	2.5	1.9
<b>Dual TEG with Heat Exchanger</b>					
<b>A-25</b>	35.26	114.89	-0.10	3.3	3.2
<b>A-100</b>	103.00	434.31	1.77	2.6	4.4
<b>B-62</b>	67.76	334.72	2.59	2.2	4.9
<b>B-100</b>	111.68	522.76	0.06	2.3	2.4
<b>C-100</b>	113.31	521.23	0.33	2.4	2.7
<b>6 TEGs on Exhaust Ports (30 cm Length)</b>					
<b>A-25</b>	20.27	112.51	-2.16	2.7	-0.2
<b>A-100</b>	64.31	398.24	-6.69	2.4	-5.0
<b>B-62</b>	39.67	329.19	0.89	1.8	2.2
<b>B-100</b>	67.99	491.93	-5.84	2.0	-4.4
<b>C-100</b>	65.00	518.56	-0.18	1.8	1.2

Table 17 lists the TEG energy input rate, WAVE BHP for each configuration, the percent difference between each configuration's BHP and the baseline model, and the BSFC improvement calculated with both the old and new equations. Immediately obvious is the possibility to have a negative BSFC improvement percentage. This happens when the power from the thermoelectric conversion to mechanical work is insufficient to offset any engine power loss due to the addition of the TEG. Above all this is seen in the case of the 6 TEGs concept where only two of the five operating points report an improvement in BSFC.

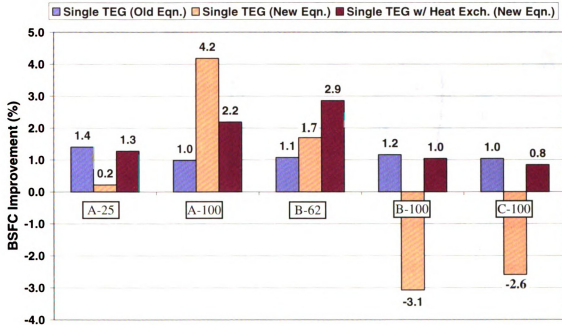


**Figure 32: Comparison of BSFC percent improvement: Single TEG/EGR cooler concept with and without heat exchanger**

Figure 32 above graphically illustrates the BSFC improvement for the single TEG/EGR cooler concept, including the new and old BSFC equation and the inclusion of the heat

exchanger after the TEG in the EGR circuit. It is quite obvious from this graph that the lower horsepower output of the single TEG/EGR cooler model at the B-100 and C-100 operating points noticeably impacts the BSFC improvement percentage. It can also be seen in Figure 32 that when the heat exchanger is added after the TEG in the EGR circuit, the engine horsepower is increased and even though there is less TEG input energy the BSFC improves.

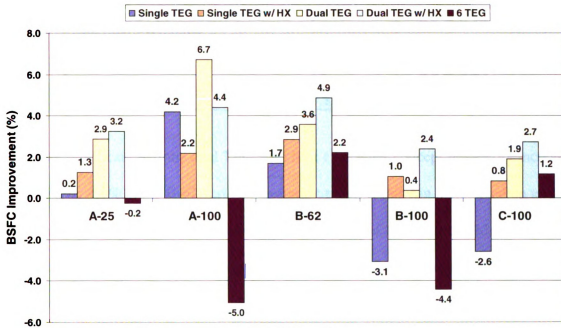


**Figure 33: BSFC percent improvement for all five concepts using new BSFC calculation**

All of the concepts discussed previously are compared in Figure 33 using the new BSFC improvement equation. This graph demonstrates dramatically how the 6 TEGs on exhaust ports concept does very little to improve BSFC. This is further reinforced when looking at the average BSFC improvement listed below in Table 18. The 6 TEGs on exhaust ports concept shows a -1.3% improvement in BSFC which indicates that overall this concept would not be a good fit for this project. Also, from this table, the dual TEG with the heat exchanger concept decidedly is the best overall concept for the average increase in BSFC.

In addition this concept also has the highest improvement in BSFC at the B-62 load point, which is the most critical load point for real world engine operation, with nearly 5% improvement in BSFC.

**Table 18: Summary of BSFC percent improvement**

<b>Concept</b>	<b>Average Operating Point BSFC Improvement (%)</b>	<b>Max BSFC Improvement (%)</b>
<b>Single TEG / EGR Cooler</b>	0.1	<b>4.2 @ A-100</b>
<b>Single TEG / EGR Cooler with Heat Exchanger</b>	1.6	<b>2.9 @ B-62</b>
<b>Dual TEG</b>	3.1	<b>6.7 @ A-100</b>
<b>Dual TEG with Heat Exchanger</b>	3.5	<b>4.9 @ B-62</b>
<b>6 TEGs on Exhaust Ports</b>	-1.3	<b>2.2 @ B-62</b>

It is quite significant that the dual TEG with heat exchanger concept reportedly increases the BSFC by 4.9% at the B-62 “cruise” operating point. If this can be realized on an ISX engine in a class 8 truck over the emissions useful life of the engine (435,000 miles) it will potentially reduce the fuel usage by 4200 gallons. It can be assumed that fuel will continue to be at least \$4.00/gallon and the reduced fuel consumption will save the operator of the truck \$17,000 or potentially more as fuel costs increase.

### **3.3.8 Summary of Phase III**

Phase III explored multiple TEG placement possibilities and went on to compare the percent BSFC improvement of these various concepts. In the process of comparing these concepts, it was realized that the previous equation for calculating BSFC improvement proved insufficient for making comparisons between concepts with differing engine power levels. A new equation was developed which incorporates a baseline power level that compensates for increases and decreases in crankshaft horsepower in the model. A new baseline model was developed which used a heat exchanger model in place of the TEG in the single TEG/EGR cooler concept which was developed in Phase II. This new baseline model was a very good match for the Cummins test data. The BSFC percent improvement was recalculated for all concepts investigated. It was realized that the dual TEG with heat exchanger concept provided the greatest improvement in BSFC, and moreover the highest BSFC improvement was seen at the B-62 load point where the engine will operate most of its useful life.

#### **4 Overall Summary**

It has been demonstrated that the use of WAVE can be a useful tool in predicting the performance of thermoelectric generators and assisting with their design.

Phase I demonstrates the potential benefits of thermoelectric generators to capture and convert waste heat energy to electricity. Phase I focused on the B-62 operating point, which simulates the typical highway cruising condition. Several assumptions were made to obtain a “best case scenario” prediction of the improvement to BSFC. Extensive studies determined the optimal combination of inner diameter and length of the TEG for performance and packaging with the Cummins ISX engine. The predicted improvement for the one, three, and six cylinders per TEG configurations were 6.2, 4.0, and 2.8% respectively. The one cylinder per TEG shows the most promise, not only in the percent improvement in BSFC but also as a model to be used in conjunction with a single cylinder test engine.

Phase II expanded upon the modeling conducted in Phase I by recreating the Cummins ISX engine in greater detail. The model now includes a full intake and exhaust system utilizing an intercooler and a VGT. Also included was an EGR circuit which had the heat exchanger section replaced with a TEG. Associated control systems for the EGR fraction and the VGT rack position were also implemented. This phase examined performance at all five operating points, and the performance of the model was shown to match up with Cummins test data to within 10% in all but one area. TEG wall temperatures were collected and TEG efficiencies were predicted. BSFC improvement was estimated in the 1.0 to 1.4% range for the five operating points.

The detailed model of the ISX engine from Phase II was modified for further studies examining possible locations for TEG placement in Phase III. The placement concepts examined included: a dual TEG concept with a secondary TEG after the turbocharger in the exhaust, a revisit of the Phase I one cylinder per TEG concept, and the modification of the Phase II and the dual TEG concepts which included a heat exchanger in the EGR circuit to improve engine performance. The BSFC percent improvement calculation was reevaluated and modified to incorporate a baseline horsepower number to achieve a more consistent comparison between different configurations. As part of the improved BSFC calculation, a baseline engine model was developed without a TEG anywhere in the exhaust system. The single TEG/EGR cooler and dual TEG concepts each with and without heat exchangers and the six TEGs on exhaust ports concept then had their respective BSFC percent improvement recalculated with the updated calculation. It was shown that on the average of all operating points the six TEGs configuration would decrease the BSFC by 1.3%, with a maximum improvement of only 2.2%. The single and dual TEG concepts both experienced an improvement in BSFC once a heat exchanger was incorporated into the EGR circuit. The dual TEG with heat exchanger was the most promising, with the average BSFC improvement of 3.5% for the five operating points. This configuration also exhibited the highest improvement at the B-62 load point of 4.9%. The six TEG concept may prove useful when used with a single cylinder test engine yet. The concept which will be most likely implemented on a production ISX engine will be the dual TEG with a heat exchanger.

## **5 Conclusion**

As transportation fuel costs continue to increase, efficient powertrain systems are more important than ever before. Efficiency includes reducing losses of energy wherever possible. Approximately 60% of fuel energy is lost as heat in a modern internal combustion engine. The use of thermoelectric generators in the exhaust system will help reduce these losses and consequently increase efficiency. The dual TEG with a heat exchanger concept will provide 4.9% better BSFC at the B-62 load point and potentially save over 4200 gallons of fuel over the emissions useful life of the engine. With fuel at \$4.00/gallon that will amount to a reduction of operating costs of over \$17,000 for the emissions useful life of 435,000 miles. This technology shows a good deal of potential for improving the fuel consumption of an over-the-road truck engine.

## **6 Future Work**

This project has several options for future work. The WAVE model can be coupled into an advanced 3D heat transfer model developed by Tom Shih at Iowa State University. The software used by Tim Hogan's group to predict TE efficiency could be coupled into the WAVE code to provide material efficiencies along the entire length of the TEG. The EGR fraction and fuel rate can be increased to match what Cummins estimates will be necessary to meet the new 2010 emission regulations. Once a TEG prototype is developed the, test data can be used to calibrate a TEG performance model which can then be coupled to WAVE.

## APPENDIX: VARIABLE GEOMETRY TURBINE MAPS

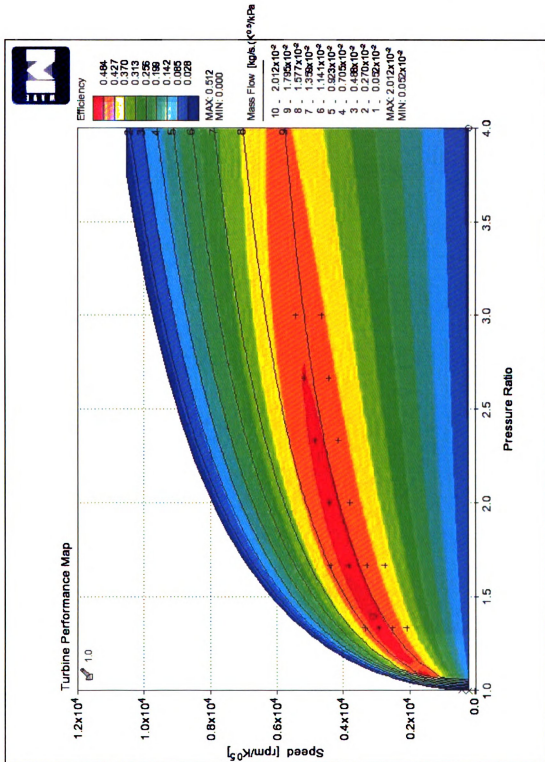


Figure 34: Turbine Performance Map VGT Rack Position 1.0

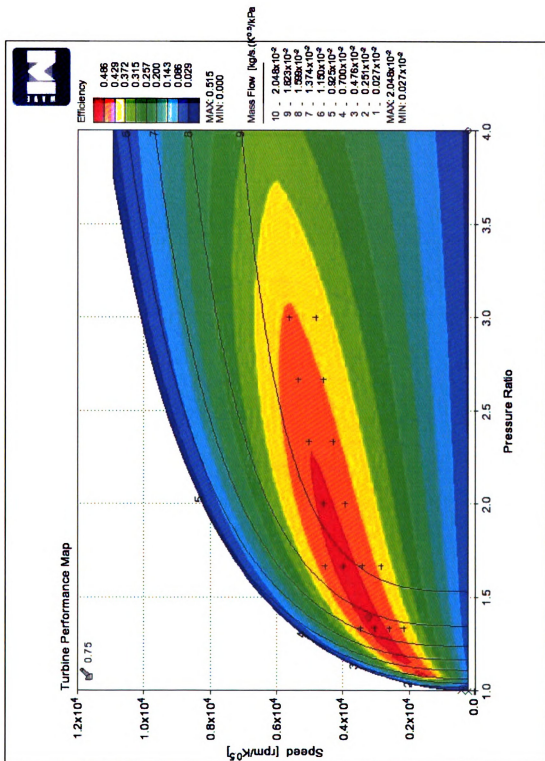


Figure 35: Turbine Performance Map VGT Rack Position 0.75

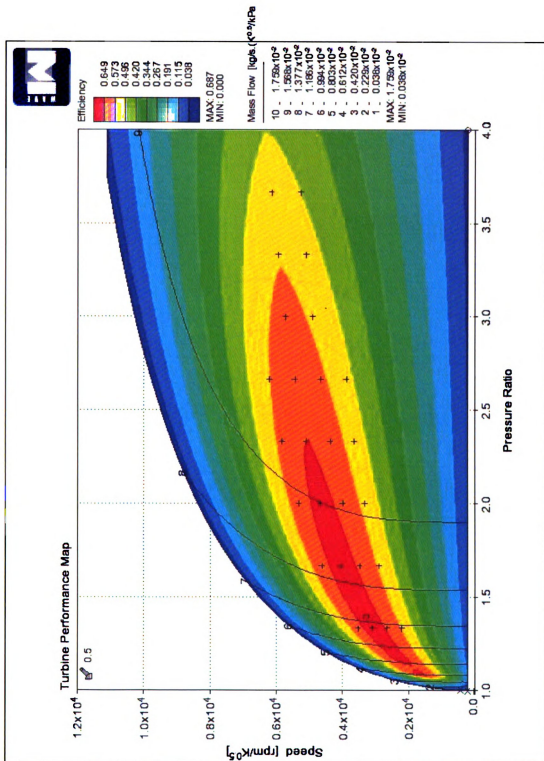


Figure 36: Turbine Performance Map VGT Rack Position 0.5

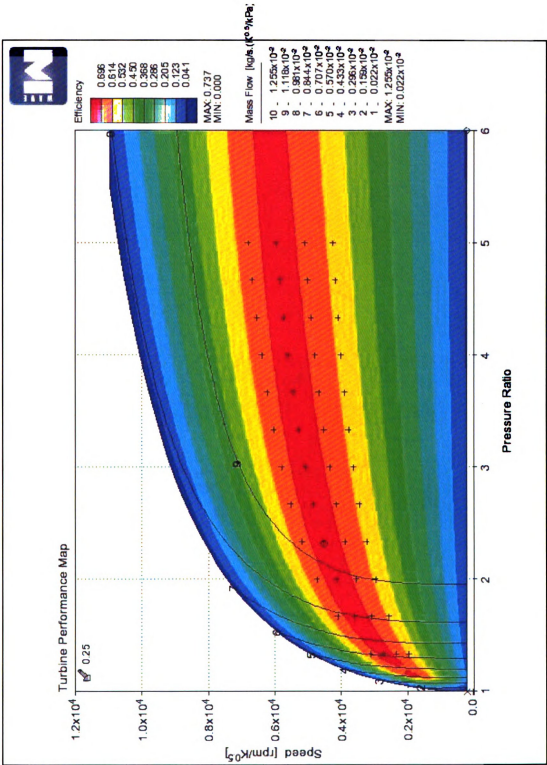


Figure 37: Turbine Performance Map VGT Rack Position 0.25



## REFERENCES

- [1] A.S. Kushch, Proc. of the 20<sup>th</sup> Intl. Conf. on Thermoelectrics, 2001, Beijing, China, pages 422-430.
- [2] K. Ikoma, Proc. of the 13<sup>th</sup> Intl. Conf. on Thermoelectrics, 1998, Nagoya, Japan 464-467.
- [3] K. Matsubara, Proc. of the 21<sup>st</sup> Intl. Conf. on Thermoelectrics, 2002, Long Beach, CA, USA.
- [4] J. Vazquez, Proc. 7<sup>th</sup> European Workshop on Thermoelectrics, 2002, Pamplona, Spain.
- [5] G. L. Bennett, CRC Handbook of Thermoelectrics, Ed. D. M. Rowe, CRC Press LLC, Boca Raton, FL, 1995.
- [6] Michigan State University et al., Thermoelectric Conversion of Waste Heat to Electricity in an IC Engine Powered Vehicle: Phase I Final Report, Department of Energy, October 2005.
- [7] Ricardo WAVE<sup>TM</sup> Basic User Manual. Release 7.2. October 2006
- [8] Ricardo WAVE<sup>TM</sup> Engine User Manual. Release 7.2. October 2006
- [9] Ricardo WAVE<sup>TM</sup> Conduction User Manual. Release 7.2. October 2006

MICHIGAN STATE UNIVERSITY LIBRARIES



3 1293 03062 5036